引用格式：申发磊，李冠奇，霍雪艺，等.Ni-Ti基形状记忆合金相变行为与弹热效应：从马氏体相变、应变玻璃转变到性能调控[J].材料工程，2026，54(8)：216-233.
SHEN Falei，LI Guanqi，HUO Xueyi，et al.Phase transformations and elastocaloric effects in Ni-Ti-based shape memory alloys：from martensitic transformation and strain glass transition to performance regulation[J].Journal of Materials Engineering，2026，54(8)：216-233.

Ni-Ti基形状记忆合金相变行为与弹热效应：从马氏体相变、应变玻璃转变到性能调控

申发磊[1]，李冠奇[1,2]，霍雪艺[1,2]，张昌硕[1,2]，张林燕[1]，王春逸[1,2]，王赵正[1,2]，郑天旭[3]，刘舒昕[4]，王鹏飞[4]，郑明晔[4]，翁　俊[4]，赵新青[2]，侯慧龙[1,2*]
（1 北京航空航天大学 天目山实验室，杭州 311115；2 北京航空航天大学 材料科学与工程学院，北京 100191；3 云南省贵金属新材料控股集团股份有限公司，昆明 650106；4 北京无线电测量研究所，北京 100854）

摘要：基于Ni-Ti基形状记忆合金晶体结构相变的弹热制冷技术具有高效、节能、环保等优势，有望替代传统蒸气压缩制冷。然而，其弹热性能的关键指标如高绝热温变、高材料性能系数、高疲劳抗力和宽工作温窗难以同时实现，制约了该技术的研发进程。本文系统介绍了Ni-Ti基形状记忆合金的制备工艺、微结构特征、相变行为与弹热性能之间的内在联系与研究进展。首先，对比分析了传统制造与增材制造工艺的特点及其对材料组织与性能的影响；其次，从晶粒形貌、析出相、孪晶等亚结构的角度，探讨了微结构对热弹性马氏体相变与缺陷诱导应变玻璃转变的调控机制；再次，阐述了不同相变路径对应的弹热效应主控参数，并总结了提升材料综合制冷性能的技术途径。最后，展望了未来可能的研究方向：通过工艺创新与新合金设计，协调热弹性马氏体相变和应变玻璃转变，实现弹热性能的协同优化；结合结构设计进一步提升换热效率、降低驱动能耗并增强工况适应性。

关键词：形状记忆合金；马氏体相变；应变玻璃转变；弹热效应
doi：10.11868/j.issn.1001-4381.2026.000055　**CSTR**：32421.14.j.issn.1001-4381.2026.000055
中图分类号：TG139^{+}.6　**文献标识码**：A　**文章编号**：1001-4381(2026)08-0216-18

Phase transformations and elastocaloric effects in Ni-Ti-based shape memory alloys: from martensitic transformation and strain glass transition to performance regulation

SHEN Falei[1]，LI Guanqi[1,2]，HUO Xueyi[1,2]，ZHANG Changshuo[1,2]，ZHANG Linyan[1]，WANG Chunyi[1,2]，WANG Zhaozheng[1,2]，ZHENG Tianxu[3]，LIU Shuxin[4]，WANG Pengfei[4]，ZHENG Mingye[4]，WENG Jun[4]，ZHAO Xinqing[2]，HOU Huilong[1,2*]
（1 Tianmushan Laboratory，Beihang University，Hangzhou 311115，China；2 School of Materials Science and Engineering，Beihang University，Beijing 100191，China；3 Sino-Platinum Metals Co.，Ltd.，Kunming 650106，China；4 Beijing Institute of Radio Measurement，Beijing 100854，China）

Abstract：Elastocaloric cooling technology，which relies on the crystal structural phase transformation of Ni-Ti-based shape memory alloys，offers advantages such as high efficiency，energy saving，and environmental friendliness. These advantages establish it as a promising alternative to conventional vapor-compression refrigeration. Large adiabatic temperature changes，high material coefficient of performance，excellent fatigue resistance，and a wide operating temperature window are critical indicators of elastocaloric performance，attaining all of these simultaneously remains challenging. This bottleneck has constrained the practical development of the technology. This review systematically introduces the intrinsic relationships and research progress among the manufacturing processes，microstructures，phase transformations，and

elastocaloric properties of Ni-Ti-based shape memory alloys. Firstly, it compares conventional and additive manufacturing processes, analyzing their effects on material microstructures and performance. Secondly, from the perspective of substructural features such as grain morphology, precipitates, and twins, it discusses the mechanism by which the microstructure regulates both the thermoelastic martensitic transformation and the defect-induced strain glass transition. Subsequently, the review elaborates on the primary controlling parameters of the elastocaloric effect across different phase transformation pathways, and summarizes technical approaches to enhance overall cooling performance. Finally, this review outlines future research directions: coordinating thermoelastic martensitic transformation and strain glass transition through process innovation and novel alloy design to achieve synergistic optimization of elastocaloric properties; and combining structural design to further enhance heat transfer efficiency, reduce driving energy consumption, and improve adaptability to operating conditions.

Key words: shape memory alloy; martensitic transformation; strain glass transition; elastocaloric effect

制冷技术的能源消耗占世界能源总需求的30%左右,且这一比例正在持续上升[1]。目前应用最广泛的传统蒸汽压缩制冷技术的能耗高、噪声大,且会破坏臭氧层和造成温室效应。因此,亟须开发节能环保的新型制冷技术。固态相变制冷技术包括弹热制冷、压热制冷、电热制冷和磁热制冷,通过施加或改变外场源产生热效应来实现制冷[2]。作为一种新兴的传统制冷技术替代方案,固态相变制冷技术具有能源效率更高、噪声污染更低和碳足迹更小等优势。美国能源部在2014年的报告中指出,与其他室温制冷技术相比,固态相变制冷中的弹热制冷技术具有最大的应用潜力[1]。

弹热材料是弹热制冷技术的核心,其中,兼具形状记忆效应、超弹性和弹热效应的形状记忆合金得到了广泛关注[3]。以Ni-Ti基形状记忆合金的热弹性马氏体相变为例,其特征相变温度与测试环境温度的差异是获得形状记忆效应/超弹性/弹热效应的主要影响因素。形状记忆效应是指在测试温度低于材料的奥氏体相变开始温度(A_s)时,材料处于马氏体状态并在加载后发生重取向,宏观上保留变形;当加热至奥氏体相变结束温度(A_f)以上时发生逆相变,宏观上自发恢复原始形状。超弹性和弹热效应是指材料在A_f温度以上加载时,应力诱发奥氏体向马氏体转变并向周围环境释放热量;卸载时的逆相变会使材料原位复原并吸收热量。通过重复此循环,可实现弹热制冷过程。当前,用于弹热制冷领域的弹热合金主要为Cu基、铁磁基、Fe基和Ni-Ti基形状记忆合金:Cu基合金具有低成本、宽工作温窗和高导热的优点[4-5];铁磁基形状记忆合金具有高的绝热温变[6-7];Fe基合金的优势在于低相变驱动力和窄相变滞后[8-9];Ni-Ti基合金兼具高绝热温变和高疲劳寿命[10-11]。然而,现有弹热合金的弹热制冷应用仍面临一些挑战,以目前研究最深入的Ni-Ti基合金为例:评估弹热效应的关键指标如高绝热温变、低能量损耗、宽工作温窗和高制冷效率等仍难以兼得[11]。

本文综述了Ni-Ti基形状记忆合金的制造工艺、微结构、相变过程与弹热效应的最新研究进展,介绍了Ni-Ti基合金不同制造工艺的特点,从晶粒形貌、析出相、位错、孪晶与胞状组织等亚结构的角度总结了微结构对马氏体相变和缺陷诱导的应变玻璃转变的影响规律,并介绍了不同相变过程对应的弹热效应指标以及提升材料制冷能力的方法,最后讨论了弹热效应的未来发展和应用方向。

1 Ni-Ti基形状记忆合金的成型工艺

1.1 传统制造

传统制造工艺如熔炼法包括真空感应熔炼和真空电弧重熔,主要通过高温熔化Ni、Ti等元素实现合金化制备Ni-Ti基形状记忆合金。在真空感应熔炼过程中,成分控制是目前的主要技术难点,例如,Ni-Ti合金中Ti元素具有较高化学活性,熔炼过程中容易与坩埚中杂质元素C、O等反应生成TiC、TiO_2和$NiTi_2$/$Ni_2Ti_4O_x$等脆性相,劣化其功/性能[12]。相比于真空感应熔炼,真空电弧重熔避免了坩埚污染,故杂质的影响相对较小,但是其相对更高的凝固速率导致成分均匀性差且凝固缺陷控制较难。由熔炼法制备的铸态形状记忆合金通常还需要进行热处理、成型加工等后处理工序,热处理工艺是为了消除铸态合金内部的残余应力,提升塑性加工能力,改善成分均匀性,但热处理工艺可能会造成合金表面氧化以及耐腐蚀性能下降[13]。热加工、冷加工成型技术能够改善合金的铸态组织,提升致密度与强度,进而提升Ni-Ti基合金的整体性能。其中,冷加工能够获得高精度尺寸与光滑表面,改善Ni-Ti基合金的超弹性行为[14]。然而冷加工

过程中可能造成加工硬化，从而导致合金的塑性降低。Ni-Ti基合金的易加工硬化和超弹性会导致严重的刀具磨损（图1(a)）[15]，使得Ni-Ti基合金的精密加工仍面临挑战。因此，传统制造的Ni-Ti基合金适用于大规模生产，经济性更高，但复杂结构成型能力弱、结构简单、功能单一（图1(b)[16]）。

1.2 增材制造

与传统制造相比，增材制造具有设计灵活、无需装配刀具或机加工、材料利用率高等优势。目前，Ni-Ti基合金的增材制造工艺主要采用铺粉式的激光粉末床熔融（laser powder bed fusion，LPBF）和送粉式的激光定向能量沉积（laser directed energy deposition，LDED）。LPBF利用激光束选择性熔化合金粉末，经快速熔凝形成非平衡微结构，其优势在于成型精度高，适用于小型复杂多孔结构的制造（图1(c)）[17]。LDED利用激光束形成熔池，通过将粉末直接喷射到熔池内部来逐层沉积，沉积速率高，更适合大尺寸简单结构件（如航空接头）的制造与修复（图1(d)）[18]。无论是LDED还是LPBF技术，其核心工艺特点在于其在熔池（毫米或微米级）尺度上实现金属粉末的快速熔化与冷却，具有极大的温度梯度（10^3～10^8 K/m）、极高的冷却速率（10^3～10^6 K/s）和复杂的熔池行为[19]，在此过程中材料经历熔化[20]、蒸发[21]、凝固[22]及析出[23]等复杂冶金过程。目前，通过高通量实验[24]、数值模拟[25]及数据驱动机器学习[26]等方法，大量的研究聚焦于能量密度、激光功率、扫描速度等工艺参数[27-28]及扫描策略[29]对成型质量、材料成分、微结构和功/性能的影响。然而，由于Ni-Ti基合金的奥氏体-马氏体相变和功/性能对打印参数非常敏感[30]，增材制造如LPBF技术对应的成型质量、成分偏析等的优化工艺窗口较窄（图1(e)[26]），目前增材制造的工艺可复现性仍较差，更适合进行小批量新材料快速开发验证和复杂结构件生产。

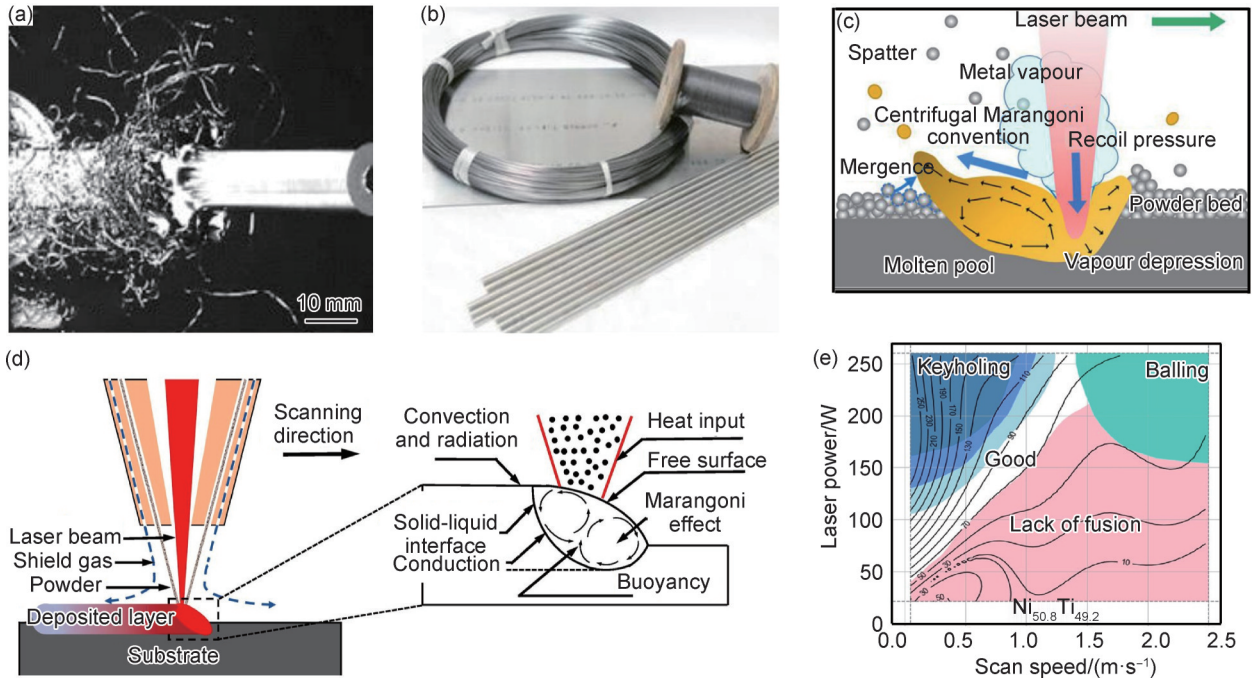


图1 传统制造和增材制造Ni-Ti基形状记忆合金的特征

(a)Ni-Ti合金的机加工缺陷[15]；(b)传统制造Ni-Ti基合金的结构形式[16]；LPBF(c)[17]和LDED(d)[18]过程及其物理现象；(e)LPBF制备$Ni_{50.8}Ti_{49.2}$（原子分数/%，下同）合金的工艺参数窗口[26]

Fig.1 Characteristics of Ni-Ti-based shape memory alloys fabricated via conventional and additive manufacturing

(a)machining defects in Ni-Ti-based alloys[15]; (b)structural configurations of conventionally manufactured Ni-Ti-based alloys[16]; LPBF(c)[17] and LDED(d)[18] process and associated physical phenomena; (e)process parameter map for the $Ni_{50.8}Ti_{49.2}$ (atom fraction, the same below) alloy fabricated via LPBF[26]

2 Ni-Ti基形状记忆合金的微结构特征及热弹性马氏体相变的调控方法

2.1 晶粒形貌特征

晶粒形貌根据纵横比可分为等轴晶粒和柱状晶粒[31]，在传统制造的Ni-Ti基合金中，其形成机制主要包括凝固、固态相变及再结晶三类。Hunt等[32-33]研究了传统铸造中柱状晶到等轴晶转变的机制，基于温度梯度、成核过冷度、凝固前沿的动态过冷度以及形核质点的数量来判定和解释柱状晶到等轴晶转变机制。

传统制造的56Ni-44Ti(质量分数/%)合金通常先通过熔炼法制成铸锭,由于缓慢的冷却速率,铸锭的显微组织通常为粗大的等轴晶粒(图2(a)[34])。为了获得性能优良的材料,通常需要对铸锭进行后续的热加工(如锻造、挤压、热轧)和冷加工(如冷轧、冷拔),并配合中间退火处理。在冷却和加热过程中,Ni-Ti基合金会在高温奥氏体和低温马氏体之间发生可逆相变,相变过程中的体积变化、界面运动(奥氏体/马氏体界面、马氏体变体间界面)和高密度位错等因素在一定程度上能够细化晶粒。再结晶过程是传统制造Ni-Ti基合金中获得细小等轴晶的最主要途径。Ni-Ti合金的再结晶温度通常为600 ℃[35],在热加工过程中,Ni-Ti铸锭会在高温(通常700~900 ℃)下进行锻造或热轧[34],粗大的等轴晶粒发生塑性变形而形成柱状的变形晶粒,并产生大量位错和畸变。由于大部分Ni-Ti基合金是难变形合金,热变形过程窗口普遍较窄,当加热温度较低时难以触发再结晶,晶粒仍为柱状的变形晶粒(图2(b)[34]);而当温度足够高时,新的、无畸变的细小等轴晶会在高畸变区域(如原晶界、孪晶界)形成并逐渐长大(图2(c)[34])。

与传统制造相比,增材制造过程中影响晶粒形貌的因素进一步增加,主要可以概括为凝固过程中的温度梯度(最大热流)方向、择优生长的晶体学方向(B2奥氏体基体相在凝固过程中沿$\langle 100\rangle_{B2}$择优生长)和"外延生长"凝固现象(扫描新一层时会对前一层进行重熔)。Gäumann等[31]改进了柱状晶到等轴晶转变的模型,使其更适合增材制造的快速凝固过程,该模型通过液固界面处的温度梯度(G)和凝固速率(R)来预测凝固组织形貌和尺寸。冷却速率($G\times R$)决定了凝固微观结构的尺寸,高冷却速率导致更细的晶粒和亚结构形成;G/R则影响凝固模式,随着G/R的降低,将依次产生平面、胞状、柱状和等轴枝晶凝固组织(图2(d))。在增材制造过程中,温度梯度的方向通常与建造方向(build direction, BD)相背,熔池的边缘区域优先冷却,随后晶粒从熔池边缘向中心生长,在此过程中温度梯度和过冷度等参数发生显著变化,结合增材制造过程中的多次热循环,增材制造Ni-Ti基合金平行于BD的截面上通常以柱状晶粒为主,且普遍存在织构[36]。以LPBF工艺为例,通过调控工艺参数(如激光功率、扫描速度和扫描间距等)和扫描策略可以改变凝固过程

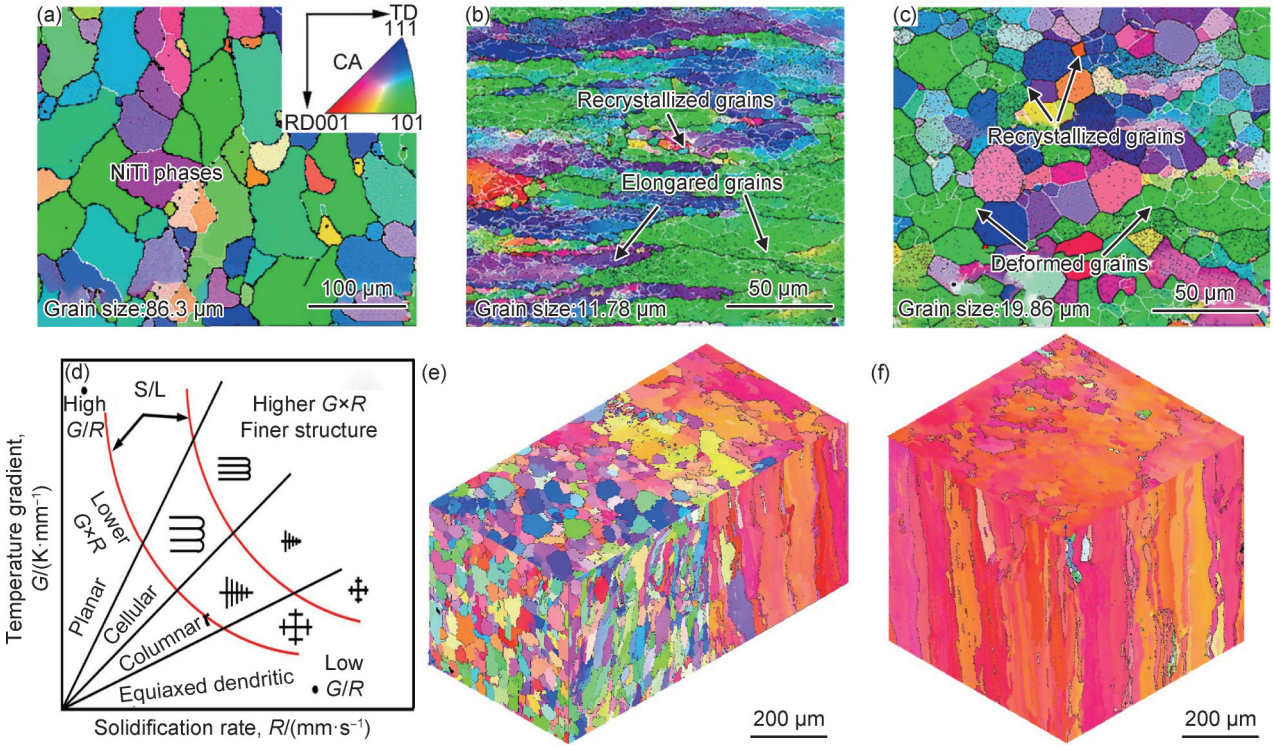


图2　传统制造和LPBF制造Ni-Ti基合金的晶粒形貌

铸造(a)、800 ℃(b)和950 ℃(c)热变形后Ni-Ti合金的晶粒形貌[34];(d)温度梯度和凝固速率对显微组织的影响[31];激光功率为400 W(e)和250 W(f)制备$Ni_{49.6}Ti_{49.4}Cu_1$合金的晶粒形貌[47]

Fig.2　Grain morphology of Ni-Ti alloys produced by conventional methods and LPBF

Grain morphology of Ni-Ti alloy after casting(a), and after thermal deformation at 800 ℃ (b) and 950 ℃ (c), respectively[34]; (d)influence of G and R on microstructure[31]; grain morphology of $Ni_{49.6}Ti_{49.4}Cu_1$ alloys fabricated with laser power of 400 W (e), and 250 W (f), respectively[47]

中的G和R从而改变局部凝固条件，实现控制晶粒的形貌和织构。通常情况下，当采用较低的激光功率和较高的扫描速度时，激光与Ni-Ti基合金粉末的相互作用时间较短，导致较大的R，抑制了晶粒生长[15]。扫描间距越小，〈001〉//BD织构越强[36-37]，这归因于低扫描间距增加了熔道数量并降低了$G\times R$，故作用到凝固层的温度更高[37-38]。通过调控扫描策略也可以控制G和R，例如Chen等[39]发现随着层间旋转角度(0°、45°、60°、67°和90°)从0°增加到90°，晶粒形貌由粗大柱状晶转变为细柱状晶和等轴晶，织构强度先增大后减小。现有研究中虽然已经实现了柱状晶强/弱织构的控制，然而，柱状晶引发的力学性能各向异性导致在一些应用场景(如多向承载工况)下的性能稳定性难以保证[40]。传统铸造工艺一般通过添加高熔点颗粒[41-43]或实施热机械处理[44]获得等轴晶，但类似传统工艺的等轴晶形成机制在增材制造Ni-Ti基合金中仍非常困难。等轴晶形成可能源于凝固、固态相变及再结晶三类机制：前者可通过添加形核剂[45]提升形核率或降低G/R[46]实现，后两者因增材制造的快速冷却特性导致扩散控制型相变与再结晶时间不足而很少发生[39]。考虑到增材制造多层成型固有的热循环效应可能在特定工艺参数下为已凝固层提供足够的温度条件与保温时间，从而触发包括再结晶在内的固态转变。Shen等[47]最近通过工艺参数调控LPBF过程中的凝固、变形和热循环实现了大范围的原位再结晶(中心区域可达90%)，形成了由具有〈001〉//BD强织构奥氏体柱状晶的边缘区域到具有弱织构等轴晶(含马氏体)的中心区域的独特梯度组织(图2(e)，(f))，并进一步阐明了利用奥氏体-马氏体之间的杨氏模量和临界应力差异实现相变顺序的可控机理。

2.2 析出相特征

Ni-Ti基形状记忆合金中的局部区域诱导析出相析出可作为同时提高强度和塑性的一种有效手段[48]，但析出相类型、尺寸和分布特征与制备工艺密切相关。在传统制造中，富Ti相($NiTi_2$/$Ni_2Ti_4O_x$)通常在Ni-Ti合金(包括富Ni和富Ti)中为脆性微米级析出相，且偏向于沿晶界分布，促进加载过程中裂纹的形成，对力学性能不利[49-51]；同时，该相的形成会消耗基体中的Ti含量，降低相变温度和减少发生马氏体相变的基体材料量[52]。但在增材制造工艺尤其是LPBF中，富Ti相在Ni-Ti合金(尤其是富Ni)中通常为纳米级尺寸并均匀分布在基体中，与基体具有共格/半共格关系，起强化作用且通常对超弹性有利[53]。根据Ni-Ti二元相图，Ni-Ti基体中还会析出Ni_4Ti_3、Ni_3Ti_2和Ni_3Ti等富Ni相。其中Ni_4Ti_3和Ni_3Ti_2相为亚稳相，即使在基体Ni含量较低的情况下，通过提高时效温度、延长时效时间等，也会逐步发生Ni_4Ti_3-Ni_3Ti_2-Ni_3Ti相的转变[54]。Lv等[55]通过真空电弧重熔重熔高纯度的Ni(99.99%)和Ti(99.99%)制备了$Ni_{55}Ti_{45}$合金，并在背散射电子成像下发现亮色的球状Ni_3Ti、板状Ni_3Ti_2、针状Ni_4Ti_3和暗色的球状Ti_2Ni析出相(图3(a))；Hou等[56]通过LDED制备的$Ni_{51.5}Ti_{48.5}$中发现大量的Ni_3Ti相(图3(b))。而由于LPBF过程中的高冷却速率、局部成分不均匀和原位快速热处理等特点，富Ni析出相在LPBF制造的Ni-Ti合金中较少被报道，这可能有以下原因：现有LPBF Ni-Ti合金大都采用微富Ni的Ni-Ti粉末，且Ni元素在LPBF过程中会优先蒸发；Ni元素在基体中的溶解度相比Ti元素更高；相对容易形成的Ni_4Ti_3相尺寸非常小而难以被观察到。Shen等[57-58]通过LPBF制备的$Ni_{50.66}Ti_{49.34}$合金中仅存在纳米级的$NiTi_2$/$Ni_2Ti_4O_x$相(图3(c))[57]；而该团队在LPBF制备的$Ni_{51.02}Ti_{48.98}$合金中发现纳米级的$NiTi_2$/$Ni_2Ti_4O_x$相和少量沿熔池中心和边缘分布的Ni_3Ti相(图3(d))，并从元素蒸发造成的反冲压力、马兰戈尼热流驱动的元素偏析解释了Ni_3Ti相的析出机制(图3(e))[58]。

2.3 位错、孪晶及胞状组织等亚结构特征

传统制造并经过热处理的Ni-Ti基形状记忆合金中位错密度通常很低，位错的引入需要采用冷加工成型等技术，且位错密度与变形量密切相关，如图4(a)所示[59]。相较而言，增材制造过程的快热快冷机制和复杂熔池行为会产生独特的亚结构，包括高密度位错、孪晶(图4(b)[60])及胞状组织(图4(c)[61])等，这些亚结构对Ni-Ti合金的功/性能有重要影响。位错的形成主要与增材制造过程中复杂热历史产生的残余应力有关，尤其是不同区域快速加热发生热膨胀和凝固收缩时的不同步被认为是位错形成的主要原因[62]。通常情况下，增材制造的工艺参数会显著改变位错密度，例如增加扫描速度会加速冷却，从而增加位错密度[63]；增加激光功率会增加激光能量输入，造成更高的温度梯度而增加位错密度[64]；增加扫描间距会减少重熔次数和热积累而增加位错密度[65]；层间旋转67°[66]、棋盘状扫描策略[64]、重复激光扫描策略[67]和基板预热[68]等都是降低位错密度的有效方法。由于熔池内的不同位置具有不同的热历史(包括峰值温度、温度梯度和凝固速率)，位错通常并不会均匀分布，例如激光扫描重叠区和熔池底部会具有更高的位错密度[53,65]。在早期的研究中，高密度位错会造成翘曲和开裂等打印缺陷、降低可恢复应变和屈服强度等，常常被认为是不利的。而最近关于增加位错密度得到

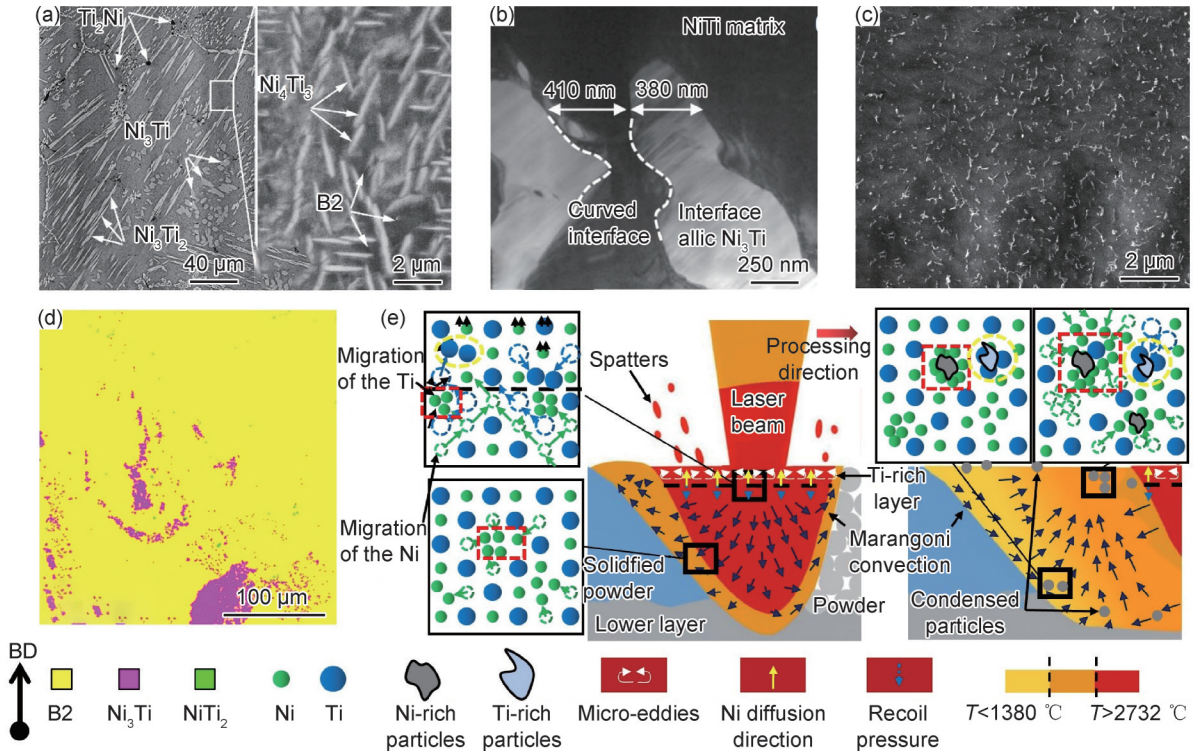


图3　传统制造和增材制造Ni-Ti合金的析出相特征与元素偏析示意图

(a)真空电弧重熔$Ni_{55}Ti_{45}$合金中的多种析出相[55]；(b)LDED制备$Ni_{51.5}Ti_{48.5}/Ni_3Ti$复合结构[56]；(c)LPBF制备$Ni_{50.6}Ti_{49.4}$合金的纳米富Ti析出相[57]；LPBF制备$Ni_{51.02}Ti_{48.98}$合金的析出相分布(d)及元素偏析示意图(e)[58]

Fig.3　Characteristics of precipitates in Ni-Ti alloys fabricated by conventional and additive manufacturing, and elemental segregation schematic

(a)various precipitates in vacuum arc melted $Ni_{55}Ti_{45}$ alloy[55]; (b)$Ni_{51.5}Ti_{48.5}/Ni_3Ti$ composite structure fabricated by LDED[56]; (c)nano-scale Ti-rich precipitates in $Ni_{50.6}Ti_{49.4}$ alloy fabricated by LPBF[57]; precipitate distribution(d) and elemental segregation schematic(e) in $Ni_{51.02}Ti_{48.98}$ alloy fabricated by LPBF[58]

的应变玻璃合金，表现出低模量、高强度、宽温域超弹性、窄滞后等功/性能，为位错密度的调控提供了新的研究方向。

Ni-Ti基合金中常存在Ⅰ型孪晶、Ⅱ型孪晶和复合孪晶三类，其中常见的Ⅰ型孪晶为$\{1\bar{1}1\}$Ⅰ型孪晶，Ⅱ型孪晶为〈011〉Ⅱ型孪晶，复合孪晶为(001)复合孪晶。当增材制造的Ni-Ti基合金在室温下为B19′马氏体相时，其内部通常由自适应的纳米孪晶组成，以协调马氏体变形，其原因可能是：(1)高的热残余应力产生应力场；(2)纳米析出相产生的局部应力场；(3)复合孪晶较小的孪生剪切变形(0.2385)易于协调孪生变形[69]。增材制造过程中产生的位错和析出相都会影响Ni-Ti基合金的孪晶类型(图4(b)[60])，但目前针对增材过程中产生的马氏体孪晶及其对功/性能的影响仍有待系统的研究。

增材制造的面心立方合金(Ni基高温合金、CoCrMo合金、AlSi10Mg和奥氏体不锈钢等)中通常会出现胞状组织，由于胞状组织对合金的屈服强度和塑性提升有很大贡献[70-71]，关于胞状组织的形成机制引起学者们的广泛兴趣。现有研究中关于胞状组织的起源主要有两方面推测：一是胞状组织通过凝固过程元素偏析引起的本征应力[60]，析出相引起的共格应变与失配位错[72]，以及枝晶间的取向差[60]而产生；另一个是凝固后的热应力引入塑性应变[73-75]而导致位错胞的形成，随后在位错壁上发生元素偏析形成胞状组织[75]。但是，其他材料如钛合金中并不出现胞状组织[47]。目前关于增材制造Ni-Ti基合金中出现胞状组织的报道也很少，Yang等[61]最近在LPBF $Ni_{51.4}Ti_{48.6}$合金中发现的胞状组织与面心立方合金中的高度相似，胞边界处为Ti元素偏析和$Ti_4Ni_2O_x$析出相，且伴随高密度位错的位错胞，如图4(c)所示。然而，现有研究中还未能解释增材制造Ni-Ti基合金中胞状组织的形成机制及其对相变和功/性能的影响，且增材制造Ni-Ti基合金的凝固模式-胞状组织-微区成分之间的关系尚不明确。

2.4　热弹性马氏体相变的调控方法

传统制造和增材制造工艺通过影响元素蒸发程度、晶粒形貌、析出相和亚结构等显著影响Ni-Ti基合金的相变过程，这归因于Ni-Ti基合金的特征相变温度对化学成分和微结构变化极为敏感，Frenzel等[76]发

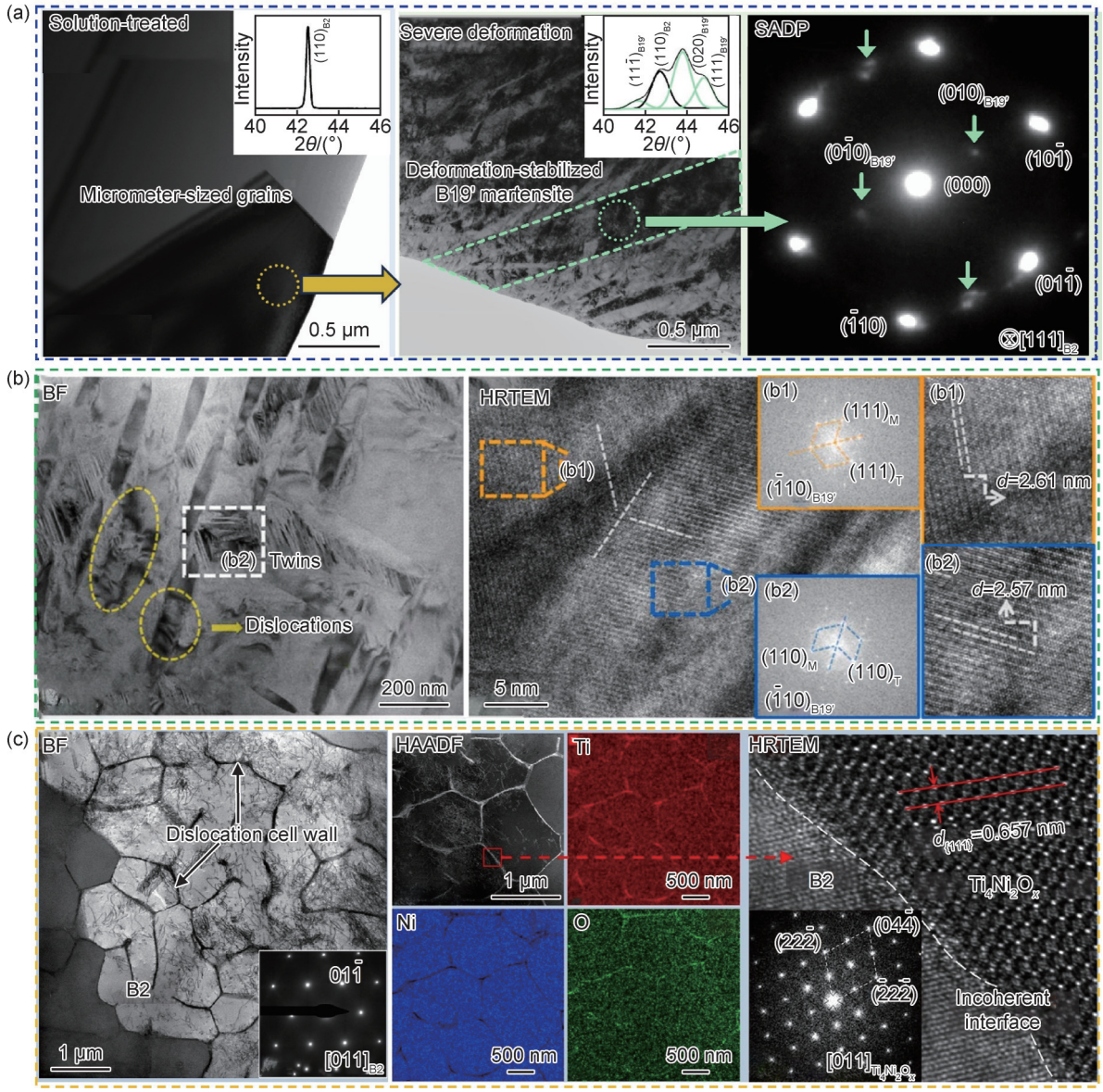


图 4 传统制造和增材制造 Ni-Ti 合金的亚结构

(a)固溶处理和严重变形后 $Ni_{50.8}Ti_{49.2}$ 合金的亚结构[59]；(b)LDED 制备 $Ni_{50.27}Ti_{49.73}$ 合金的亚结构[60]；(c)LPBF 制备 $Ni_{51.4}Ti_{48.6}$ 合金中的胞状组织[61]

Fig.4 Substructure of conventionally and additively manufactured Ni-Ti alloys

(a)substructure of a $Ni_{50.8}Ti_{49.2}$ alloy after solution treatment and severe deformation[59]; (b)substructure of a $Ni_{50.27}Ti_{49.73}$ alloy fabricated by LDED[60]; (c)cellular structure in a $Ni_{51.4}Ti_{48.6}$ alloy fabricated by LPBF[61]

现在 Ni-Ti 合金中，Ni 含量每增加 1%，相变温度降低约 83 K(图 5(a))。在增材制造过程中，通过工艺优化可以实现局部区域定制成分和微结构，进而实现相变过程的可定制。通过激光能量密度归一化主要的 LPBF 工艺参数，以 LPBF 制备 Ni-Ti 基合金为例，多数研究表明相变温度随能量密度增加而增加[77-79]，这归因于 LPBF 过程中 Ni 元素的优先蒸发[28,52]。还有研究发现，在相同能量密度但不同激光功率和扫描速度的参数组合下，相变温度也会存在显著差异[80-81]，且激光功率对元素蒸发的影响大于扫描速度[82]。Wang 等[28]发现相变温度随扫描速度和扫描间距的增加而降低，而随激光功率的增加而增加(图 5(b))，这同样与元素蒸发有关。但也有部分研究指出 Ni 元素损失并不总是比 Ti 的损失更显著，Chen 等[83]发现采用 250 W 和 40 W 制备的 Ni-Ti 合金中 Ni 含量相近，Dadbakhsh 等[84]认为相变温度的变化主要与析出相有关。针对性地添加与 Ni 或 Ti 化学性质相似元素可定向优化 Ni-Ti 基合金的相变行为和功能特性(图 5(c)[54])。例如，Cr、Fe、Co、V 等元素的添加会显著降低相变温度；Hf、Pd、Pt、Zr 元素会显著提高相变温度；Nb 会显著增

加相变滞后;Cu元素会提升相变稳定性[85]和降低相变滞后[86-87]等;Ta元素添加则会显著提升耐蚀性和X光可见性[88]。需要注意的是,现有研究大多探讨工艺参数对相变温度的影响趋势,而采用相同粉末成分和工艺参数并不意味着能得到相同的相变温度,如何掌握微区成分变化规律进而精确控制特定区域的相变温度仍是非常具有挑战性的工作。

除相变温度外,微结构特征也对Ni-Ti基合金的功/性能具有重要影响,如微区成分的不均匀性、晶粒形貌与取向织构、非平衡析出相和亚结构(位错、孪晶和胞状组织等)等。Li等[89]通过LPBF制备$Ni_{51}Ti_{49}$合金并进行700 ℃固溶+250 ℃时效两步热处理,在B2基体中建立高密度富Ni局部化学不均匀微区,并获得了优异的拉伸超弹性(图5(d));Shayesteh Moghaddam等[90]采用LPBF制备了$Ni_{50.8}Ti_{49.2}$合金,因具有[001]//BD强织构实现了5.62%的可恢复应变(恢复率达98%)(图5(e));在析出相方面,Gu等[53]发现纳米级$NiTi_2$/$Ni_2Ti_4O_x$相能提高Ni-Ti合金的屈服强度;Cao等[91]发现40~70 nm的Ni_4Ti_3析出相可以显著增强压缩超弹性(可恢复应变为4.6%)、屈服强度和循环稳定性;Hou等[56]发现在LDED制备的$Ni_{51.5}Ti_{48.5}$合金中出现的大量Ni_3Ti相会促使超弹性压缩曲线的滞后

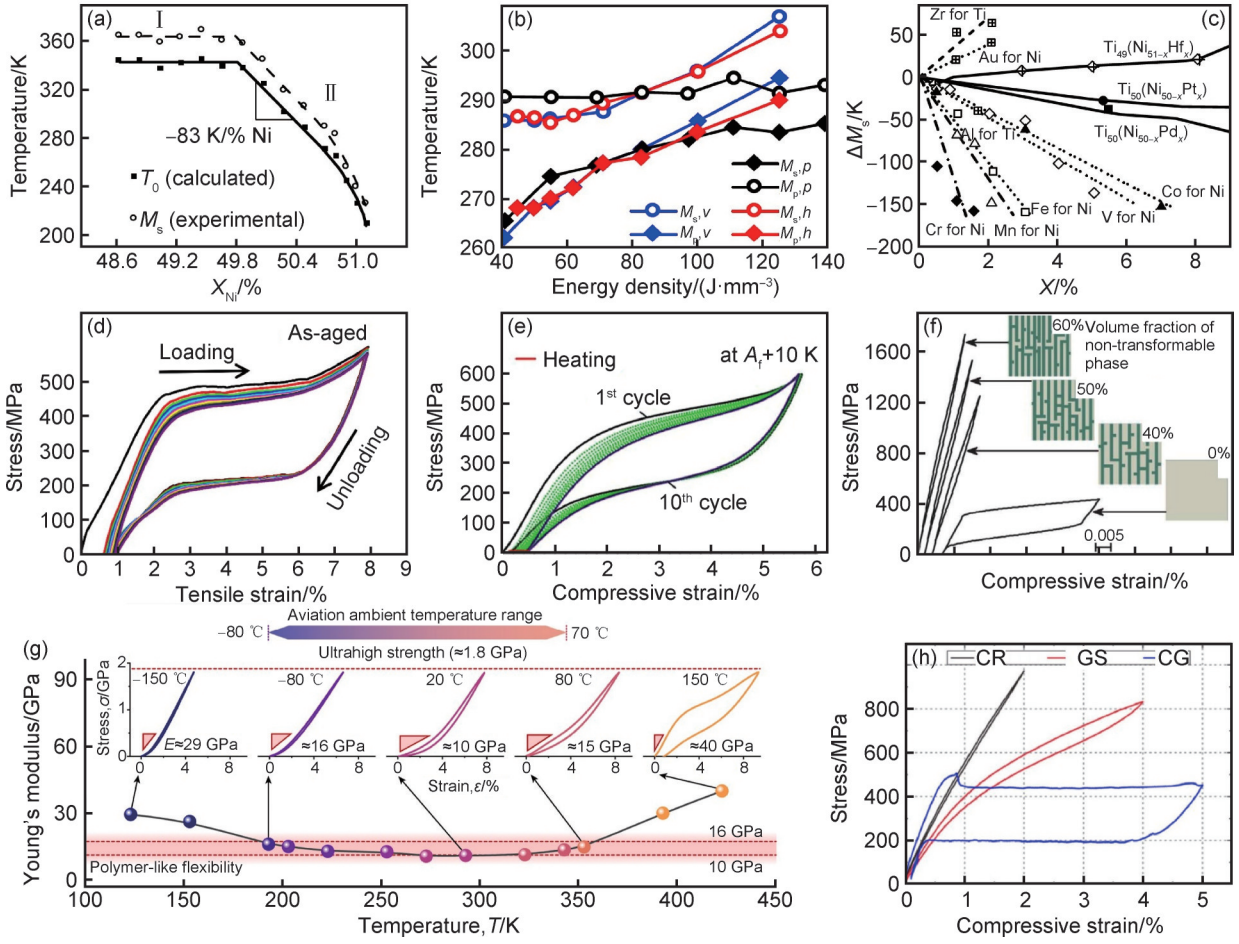


图5　传统制造和增材制造Ni-Ti基合金的相变行为和超弹性响应

(a)相变温度和Ni含量的对应关系[76];(b)相变温度与LPBF工艺参数(能量密度、激光功率P、扫描速度v和扫描间距h)的关系[28];(c)合金元素对Ni-Ti合金相变温度的影响[54];(d)LPBF制备$Ni_{51}Ti_{49}$合金并进行700 ℃+250 ℃两步热处理后的拉伸曲线[89];(e)LPBF制备强织构$Ni_{50.8}Ti_{49.2}$合金的压缩曲线[90];(f)高Ni_3Ti相含量$Ni_{51.5}Ti_{48.5}$合金的压缩曲线[56];(g)应变玻璃态$Ni_{50.8}Ti_{49.2}$合金的压缩曲线[59];(h)不同晶粒尺寸(CR:细晶,GS:粗晶+细晶,CG:粗晶)Ni-Ti合金的压缩曲线[93]

Fig.5　Phase transformation behavior and superelastic responses of Ni-Ti-based alloys fabricated by conventional and additive manufacturing

(a)correspondence between transition temperatures and Ni content[76];(b)relationship between transition temperatures and LPBF parameters (energy density,P,v,h)[28];(c)effect of alloying elements on the transition temperatures of Ni-Ti alloys[54];(d)tensile curves of the $Ni_{51}Ti_{49}$ alloy fabricated by LPBF after two-step heat treatment (700 ℃+ 250 ℃)[89];(e)compressive curves of $Ni_{50.8}Ti_{49.2}$ alloys with strong texture fabricated by LPBF[90];(f)compressive curves of $Ni_{51.5}Ti_{48.5}$ alloys with Ni_3Ti precipitates[56];(g)compressive curves of $Ni_{50.8}Ti_{49.2}$ alloys[59];(h)compressive curves of Ni-Ti alloys with different grain sizes (CR:fine-grained,GS:mixed coarse and fine grains,CG:coarse-grained)[93]

面积显著降低(图5(f))。在亚结构方面,Xu等[59]通过传统工艺(冷拉变形50%+300 ℃热处理+12%预应变)制备的$Ni_{50.8}Ti_{49.2}$合金保留了高密度位错,具有1.8 GPa的屈服强度、10.5 GPa的杨氏模量和8%的可恢复应变,且在−80~80 ℃温度范围内保持这些性能(图5(g))。孪晶行为同样会改变超弹性,尤其是LPBF过程中产生的热残余应力,通常会诱发部分奥氏体发生马氏体相变和孪晶马氏体发生重取向,这可能会增加马氏体逆相变阻力,且形成的马氏体孪晶界为位错滑移提供通道,进而导致可恢复应变降低[92],也可能作为后续相变的"种子"而使相变无需形核,降低应力滞后面积[59]。胞状组织在力学性能上的优势已在LPBF面心立方合金中被广泛报道,然而目前仍未有研究关注Ni-Ti基合金中胞状组织的形成机制及其对相变行为和功能特性的影响,其预期的作用可能类似于晶粒细化,如限制大尺寸马氏体板条的形成而减小相变滞后等(图5(h))[93]。

3 应变玻璃转变的微结构特征及调控方法

3.1 应变玻璃转变及其相变特征

在Ni-Ti基形状记忆合金中引入大量缺陷(元素掺杂、位错和析出相等)会阻碍前述马氏体相变的长程应变有序。缺陷产生的随机分布应力场限制了降温过程中长程有序马氏体的形成,取而代之发生短程有序的局部类马氏体畴的形成、长大和冻结,这一转变被称为应变玻璃转变。应变玻璃转变普遍存在于Ti-Ni基合金、β-Ti合金[94]和Heusler合金[95]等多种铁弹体系中,根据Zhang等[96]的研究总结应变玻璃转变具备如下特征:动态力学性能的频率分散性:在各玻璃系统(如弛豫铁电体、自旋玻璃和应变玻璃)中,玻璃化转变因其降温引起动态冻结的物理过程,在转变温区内通常表现出对频率的依赖性。在应变玻璃合金中,频率依赖性体现在合金的储能模量上,如图6(a)~(c)所示。合金无相变的储能模量随冷却单调增加,并遵循Wachtman方程[55,97](图6(a))。在降至玻璃化转变温区时,曲线上出现随频率弥散分布的储能模量低谷(图6(b)),其对应的温度(T_g)与频率(ω)符合Vogel-Fulcher关系见式(1)[98-99]:

$$\omega = \omega_0 \cdot \exp[E_a/(k(T_g - T_0))] \quad (1)$$

式中:T_0、T_g、E_a、ω_0和k分别表示理想冻结温度、玻璃化转变温度、活化能、预因子和玻尔兹曼常数(图6(c))。

平均晶体结构不变性:温度的降低不再引起奥氏体向马氏体的热弹性转变,合金的平均结构在各温度下始终保持为奥氏体相。如图6(d)的原位XRD结果所示,该合金在冷却过程中基体相始终为B2奥氏体,仅发生相变峰的宽化,即未发生宏观马氏体相变[100-101]。应变玻璃合金在升降温的过程中,也不再表现出一级相变所具有的吸热/放热峰,如图6(e)所示。因此用于表征马氏体相变的DSC、原位XRD等常用实验手段不适用于对应变玻璃合金的玻璃化转变温度等物性参数进行测试。

各态遍历性的破缺:冻结的玻璃系统受动力学减速的影响,不再具有各态遍历性。应变玻璃合金冻结时被限定在多重自由能低谷中的某特定微观状态,在实验观测时间范围内不转变为其他微观状态,这一特征可通过零场冷却(ZFC)/场冷却(FC)实验测试其物理性质(在应变玻璃合金中为应变)对温度-外场变化的历史依赖性进行验证。如图6(f)所示,在T_g温度以下ZFC曲线与FC曲线之间存在明显偏差,表明应变状态具有对温度-外场历史依赖性,验证了其遍历性破缺的特征(图6(f))。

类马氏体纳米畴的生长:区别于马氏体相变形成的微米级马氏体孪晶结构,应变玻璃合金随温度降低发生类马氏体纳米畴的形成、生长和冻结行为。如图6(g)~(n)所示,高分辨透射电子显微(transmission electron microscope, TEM)技术能够对应变玻璃合金内的畴演化现象进行表征,在298 K下的明场像中可以观察到典型的粗花呢图案[100,102-103](白色虚线框内),沿$[111]_{B2}$晶带轴的选区电子衍射图(图6(h)的插图)展示了由马氏体纳米畴产生的附加斑点。通过暗场像能够直接观察到这些弥散分布在B2基体中的马氏体纳米畴(图6(h))。相比298 K,冷却到100 K下的明场像显示B2基体中更明显的粗花呢图案,附加斑点的亮度也有所提高,暗场像中能够观察到纳米畴尺寸与数量的增加(图6(l))。选择图6(i),(m)中红色箭头所指的额外斑点得到反快速傅里叶变换图,可以发现随测试温度从298 K降低到100 K时,由白色虚线标记的短程有序B19′纳米畴的长大,如图6(j),(n)所示。

3.2 单一缺陷诱导应变玻璃转变

应变玻璃合金中的缺陷类型主要包括点缺陷、线缺陷和体缺陷。点缺陷(如元素掺杂)会导致其附近的晶体结构发生晶格畸变,形成单个的"应变微区"。当点缺陷浓度足够高时,这些随机分布的应变微区相互交叠,形成一个全局化的随机应变网络(图7(a)[104])。随着温度降低,该应变网络会促使短程马氏体畴在局部形核并冻结,最终形成应变玻璃。点缺陷可以通过添加第三合金元素来引入,如Ni-Ti–X体

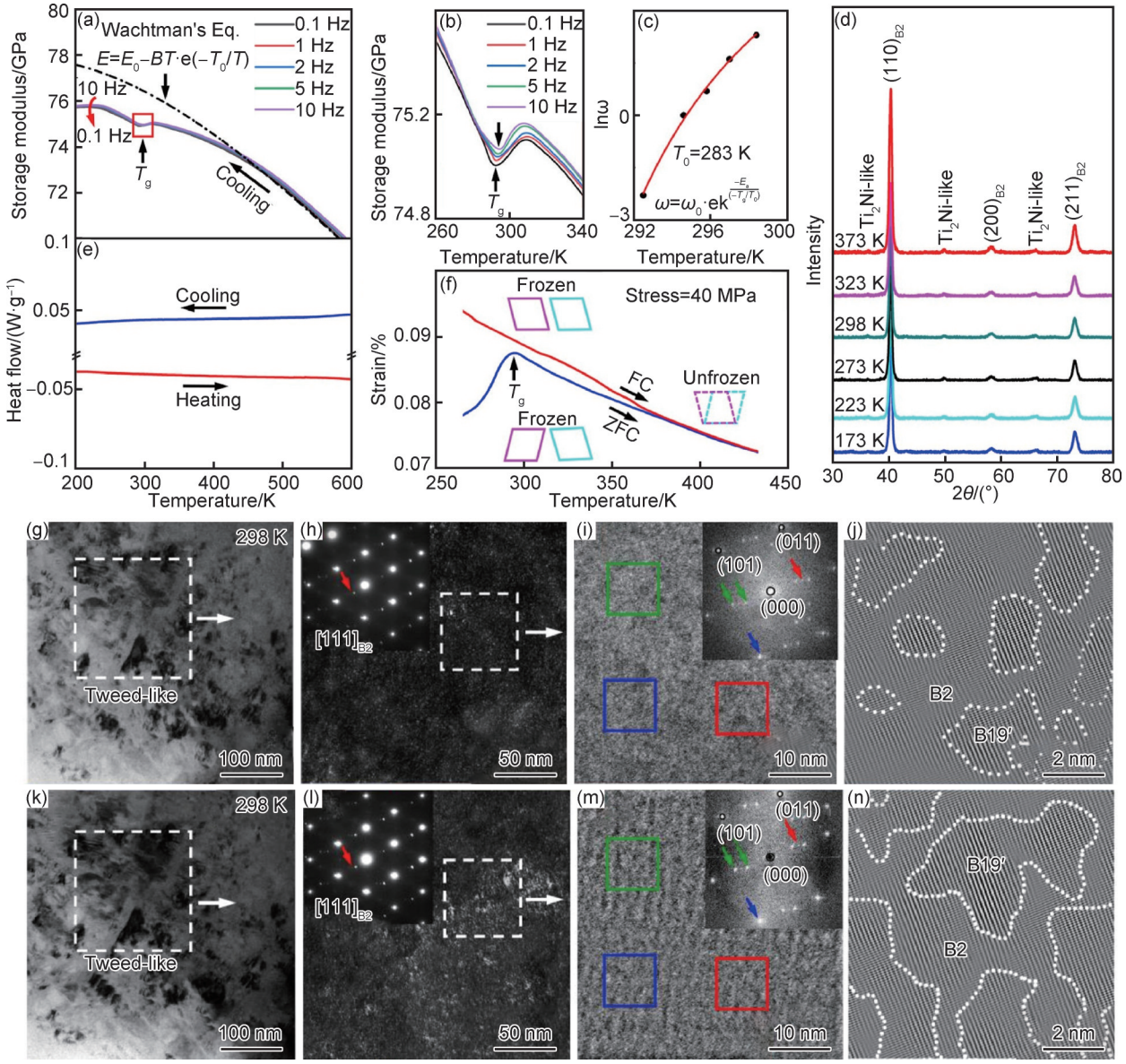


图6　$Ti_{16.6}Zr_{16.6}Hf_{16.6}Ni_{16.6}Cu_{16.6}Co_{16.6}$合金的应变玻璃转变特征[96]

(a)～(c)动态力学性能的频率分散性；(d)原位XRD结果中的平均结构不变性；(e)DSC曲线中无相变峰；(f)零场冷却/场冷却(ZFC/FC)曲线中的遍历性缺失；(g)～(n)不同温度下的原位TEM表征马氏体畴演变

Fig.6　Characteristics of strain glass transition in $Ti_{16.6}Zr_{16.6}Hf_{16.6}Ni_{16.6}Cu_{16.6}Co_{16.6}$ alloy[96]

(a)-(c)frequency dispersion of dynamic mechanical properties; (d)invariance of average structure in *in-situ* XRD results; (e)absence of transformation peaks in DSC curves; (f)ergodicity breaking in zero-field-cooled/field-cooled (ZFC/FC) curves; (g)-(n)evolution of martensitic domains characterized by *in-situ* TEM at different temperatures

系[102](其中X = Ni[105]、Fe[106]、Cu[107]、Nb[108]、Co[109]等)，这在传统制造和增材制造中都可以实现。线缺陷(如位错)的长程弹性应力场能有效地钉扎马氏体核胚，抑制其长程协作生长，从而引发应变玻璃转变[110](图7(b)[104])。在传统制造中，线缺陷主要通过热机械处理(如冷轧、冷拉等)引入，其缺陷密度与塑性变形量高度相关；增材制造过程中因快速凝固与热循环作用产生的热应力也可以产生高密度位错，且无需改变样品的几何形状和尺寸。与点缺陷类似，体缺陷(主要是纳米级析出相)产生的局部晶格畸变同样会抑制长程应变有序马氏体相变并诱导应变玻璃转变(图7(c)[104])。在传统制造中一般通过后热处理促进纳米相的析出，如低温退火促进了Ni-Ti-Zr[111]和Ni-Ti-Hf[112]合金中纳米H相的析出，从而发生应变玻璃转变。增材制造过程中的高冷却速率同样可以直接得到纳米级析出相而无需进行热处理。

点缺陷、线缺陷和体缺陷的共同点是在奥氏体基体中引入随机分布的应变源，使得宏观上不发生长程

马氏体相变，而微观上存在纳米尺度的类马氏体畴结构。然而，不同缺陷类型合金对应的微结构和性能特点显著不同。点缺陷主要通过改变电子浓度和化学键合来改变相变驱动力，这通常会显著改变相变温度（图7(e)）[113]，例如Ni元素、Fe元素和Co元素等合金化元素的掺杂能够将应变玻璃合金的超弹性工作温区拓展到低温区间（低于273 K）。而位错则主要通过长程应力场施加几何约束，不会改变基体的整体化学成分，对相变温度的影响相对较小。并且位错的引入不会减少发生相变的基体相体积分数，提高了应变玻璃合金超弹性的可恢复应变。冷轧引入的微结构特征还能够使合金具备Elinvar、Invar等特殊功能[94,114]。体缺陷（纳米析出相）的引入一方面能够引入应变玻璃转变，另一方面能够通过弥散强化机制提高位错开动和滑移所需要的激活能，提高Ni-Ti基合金在高温下的屈服强度。

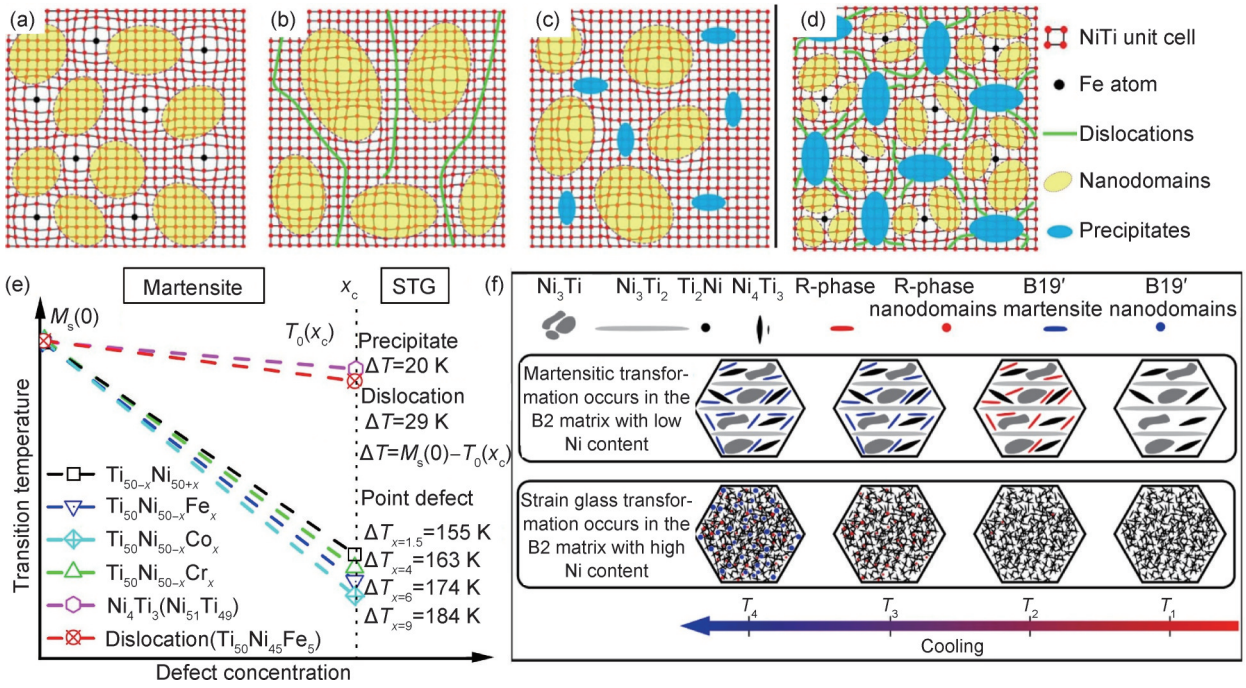


图7 应变玻璃转变的缺陷类型及其对性能的影响机理

点缺陷(a)、线缺陷(位错)(b)、体缺陷(析出相)(c)和多缺陷复合(d)诱导发生应变玻璃转变的示意图[104]；(e)单一缺陷类型对相变温度的影响规律[113]；(f)复合缺陷类型$Ni_{55}Ti_{45}$合金的相变示意图[55]

Fig.7 Defect types in strain glass transition and their influence mechanisms on properties

Schematic diagrams of the strain glass transition induced by point defects(a), line defects (dislocations)(b), volume defects (precipitates)(c), and composite defects(d)[104]; (e)effect of a single defect type on transformation temperatures[113]; (f)schematic diagram of the phase transformation in a $Ni_{55}Ti_{45}$ alloy with composite defects[55]

3.3 复合缺陷诱导应变玻璃转变

在实际材料体系中，点缺陷、线缺陷和体缺陷往往以复合形式共存（图7(d)[104]），共同决定应变玻璃与马氏体相变的竞争或耦合关系。通常情况下，传统工艺可以通过元素掺杂+热处理的方式同时引入点缺陷和体缺陷。例如，Zhang等[96]通过真空电弧重熔制备$Ti_{16.6}Zr_{16.6}Hf_{16.6}Ni_{16.6}Cu_{16.6}Co_{16.6}$高熵合金，随后在1473 K下保温12 h并水冷，发现纳米析出相（Ti_2Ni和HfO_2）诱导的局部应力/应变场结合点缺陷共同促进了应变玻璃转变。与此不同的是，Lv等[55]通过真空电弧重熔制备富Ni的$Ni_{55}Ti_{45}$合金，随后在1323 K下保温12 h并随炉冷却，发现过量Ni掺杂和热处理后不均匀分布的富Ni析出相导致同时获得了应变玻璃转变和马氏体相变特征，这与其他富Ni的$Ni_{50+x}Ti_{50-x}$（$x>1$）合金中仅出现应变玻璃显著不同[100]，意味着复合缺陷类型的复合形式对相变行为具有非常显著的影响。增材制造过程中的快速凝固和热循环会在材料中同时引入点缺陷（由于合金元素的引入和成分不均匀性）、位错（由于快速凝固导致的热应力）和体缺陷（由于快速凝固析出的纳米相）[104]，使得多种缺陷的耦合作用对相变行为的调控更为灵活：点缺陷提供应变场的基本单元，位错增强局部区域的应变场且不改变基体成分，析出相则进一步改变基体局部区域的化学成分并作为相变形核的异质核心。通过综合上述各缺陷类型的作用机制，复合缺陷型应变玻璃有望实现马氏体相变和应变玻璃转变的灵活调控。

4　弹热效应

4.1　基于马氏体相变的弹热效应

弹热效应是指材料在绝热条件下受力发生相变时,伴随温度变化的现象,其主要评价指标有绝热温变ΔT_{ad}或等温熵变、能量损耗(即应力滞后面积)、材料性能系数COP_{mat}、抗疲劳性能、工作温度窗口和驱动力等[11]。在实际应用过程中通常需要综合考虑上述指标,但在现有研究中,上述指标仍难以同时提升。在马氏体相变过程中,由于应力诱发马氏体相变和逆相变的相变应变通常高于4%,故产生较大的ΔT_{ad}($\approx$20 K)[115]。马氏体相变材料种类丰富(如Ni-Ti基、Fe基、Cu基和高熵合金等),可根据实际应用需求进行选择。然而,马氏体相变通常存在高能量损耗(图8(a))[115]、低COP_{mat}、低疲劳寿命和窄工作温度窗口等问题。为优化基于马氏体相变的弹热性能,研究者提出了多种微结构调控方法:(1)热机械处理。在细化晶粒的同时保留高密度位错和促进析出相形成。Lin等[116]通过冷轧(厚度减少38%)和退火(583 K, 2 min)制造了平均晶粒尺寸为31 nm和高密度位错(4.7×10^{15} m^{-2})的纳米晶$Ni_{50.8}Ti_{49.2}$合金,有效提高了屈服强度(2.09 GPa)和疲劳寿命(超10^6次循环),同时保留较高的ΔT_{ad}(−17.3 K)。(2)添加合金元素。如通过添加Fe[117-118]或Cu[119-120]元素可分别引入R相或B19相来调整相变温度和滞后,从而降低相变驱动力、提升COP_{mat}和抗疲劳性能。Hou等[118]发现$Ti_{50}Ni_{48.5}Fe_{1.5}$合金丝中的不均匀B2↔R相变可在不到500 MPa的驱动力下产生−5.8 K的ΔT_{ad}和超20的COP_{mat},兼具高的疲劳寿命(超10^5次循环);Chluba等[120]发现发生B2↔B19相变的Ti-Ni-Cu薄膜经10^7次循环后超弹性无明显衰减。(3)多孔结构设计。通过增加比表面积可增加材料与环境的换热面积并显著降低驱动力[121-122]。Nyabadza等[121]比较了体心立方多孔结构和实体Ni-Ti合金的弹热性能差异,发现多孔结构仅需实体Ni-Ti合金一半的驱动力即可获得相似的ΔT_{ad},且前者有利于增加比表面积以实现更有效的热交换;Peng等[123]通过LPBF制造的仿生多孔结构在149.11 N的外加应力下产生−2.3 K的ΔT_{ad}。(4)异质微结构设计。例如形成粗晶和纳米晶梯度[93]、B2↔B19′/B19/R多相变类型复合[124]、基体相和大量的强化相(Ni_3Ti、Ti_2Ni等)[22]和梯度孔隙率多孔结构[125]等,基于“区域定制功/性能”和“成分-结构一体化设计”思路提升弹热效应的综合评价指标。Zhan等[124]通过LPBF技术制备了具有交替“粗-细”晶粒尺寸的55.98Ni-44.02Ti合金,发现这种异质微结构可实现逐步梯度相变行为,相比单一相变样品的COP_{mat}提高52.3%,且ΔT_{ad}几乎不变;Hou等[56]通过LDED制备了$Ni_{51.5}Ti_{48.5}$合金,发现B2相+Ni_3Ti相复合微结构可将COP_{mat}显著提升4~7倍,并在超10^6次循环后仍能保持4 K的ΔT_{ad}。(5)其他影响因素。如加载模式(拉伸、压缩和扭转等)[126]、应变速率[127]和表面质量等也会影响上述指标。Hou等[126]从弹热合金中疲劳裂纹的萌生与扩展角度分析了引发疲劳的根本原因,并介绍了通过减少表面缺陷和利用压缩方式克服疲劳破坏的研究进展。Yao等[128]通过在弹热装置中设计能回收动能的滚轮驱动机构实现了功回收,结合Ti-Ni-Cu合金将性能系数提升了1倍。

4.2　基于应变玻璃的弹热效应

应变玻璃转变属于长程无序而短程有序的局部转变,纳米马氏体畴随温度降低而逐渐长大,在到达T_g温度附近开始冻结,在低于T_g温度后完全冻结,因此具有宽工作温度窗口的超弹性和弹热效应。同时,马氏体畴的存在导致相变过程无需形核而表现出准线性超弹性和低的能量损耗(图8(b))[96],因此COP_{mat}和抗疲劳性能都较高。然而应变玻璃合金中的高缺陷浓度会产生高的局部马氏体相变能垒,纳米马氏体畴在加载过程中无法完全转变为长程有序的马氏体[129],且高缺陷密度和纳米马氏体畴都降低了产生弹热效应的NiTi基体相体积分数。因此,目前通过应变玻璃转变获得的ΔT_{ad}($\approx$4 K,图8(e))[96]远低于马氏体相变获得的ΔT_{ad}($\approx$20 K,图8(d))[115]。

图8(g)~(i)中总结了现有研究中马氏体相变和应变玻璃转变对应的弹热性能[2,96,115,130-136],尽管现有研究中已通过调控晶粒形貌、析出相、亚结构和成分等分别获得了马氏体相变和应变玻璃转变,但单一相变过程仍无法实现弹热制冷性能的综合提升。例如,马氏体相变具有的高ΔT_{ad}对应高可恢复应变(图8(g))、低COP_{mat}(图8(h))和窄工作温度窗口(图8(i)),应变玻璃转变则刚好相反。为了实现弹热制冷性能的综合提升,通过调整合金成分和制备工艺来引入复合相变过程是有前途的研究方向之一。例如,Lv等[55]通过点缺陷(Ni掺杂)和体缺陷(富Ni析出相)的复合在$Ni_{55}Ti_{45}$合金中实现了应变玻璃转变和马氏体相变共存,在保持低能量损耗(图8(c))的同时显著提升了ΔT_{ad}($\approx$10 K,图8(f))。Chen等[133]通过冷轧后激光表面退火获得了具有梯度晶粒尺寸的Ni-Ti合金,发现梯度晶粒尺寸样品相比冷轧态样品具有更高的ΔT_{ad},相比粗晶粒样品则具有更宽的工作温度窗口(图8(i))。此外,在应变玻璃转变和马氏体相变之间还存在交叉型应变玻璃转变,对于缺陷浓度适中的交叉型应变玻

璃合金，同时具有短程和长程有序的相变特征[130]。类似于普通应变玻璃合金，交叉型应变玻璃合金的马氏体畴也可在T_g温度附近的宽温域内存在，因此也具有宽温域超弹性[131]。并且由于缺陷密度比普通应变玻璃合金更低，交叉型应变玻璃合金中可逐渐生成长程有序马氏体相，这意味着可利用更多的转变应变，从而提供比典型应变玻璃合金更大的可恢复应变[132]。尽管目前还未见交叉型应变玻璃合金弹热效应方面的研究，但交叉型应变玻璃合金在平衡高ΔT_{ad}、高COP_{mat}和宽工作温窗方面提供了新的研究思路。

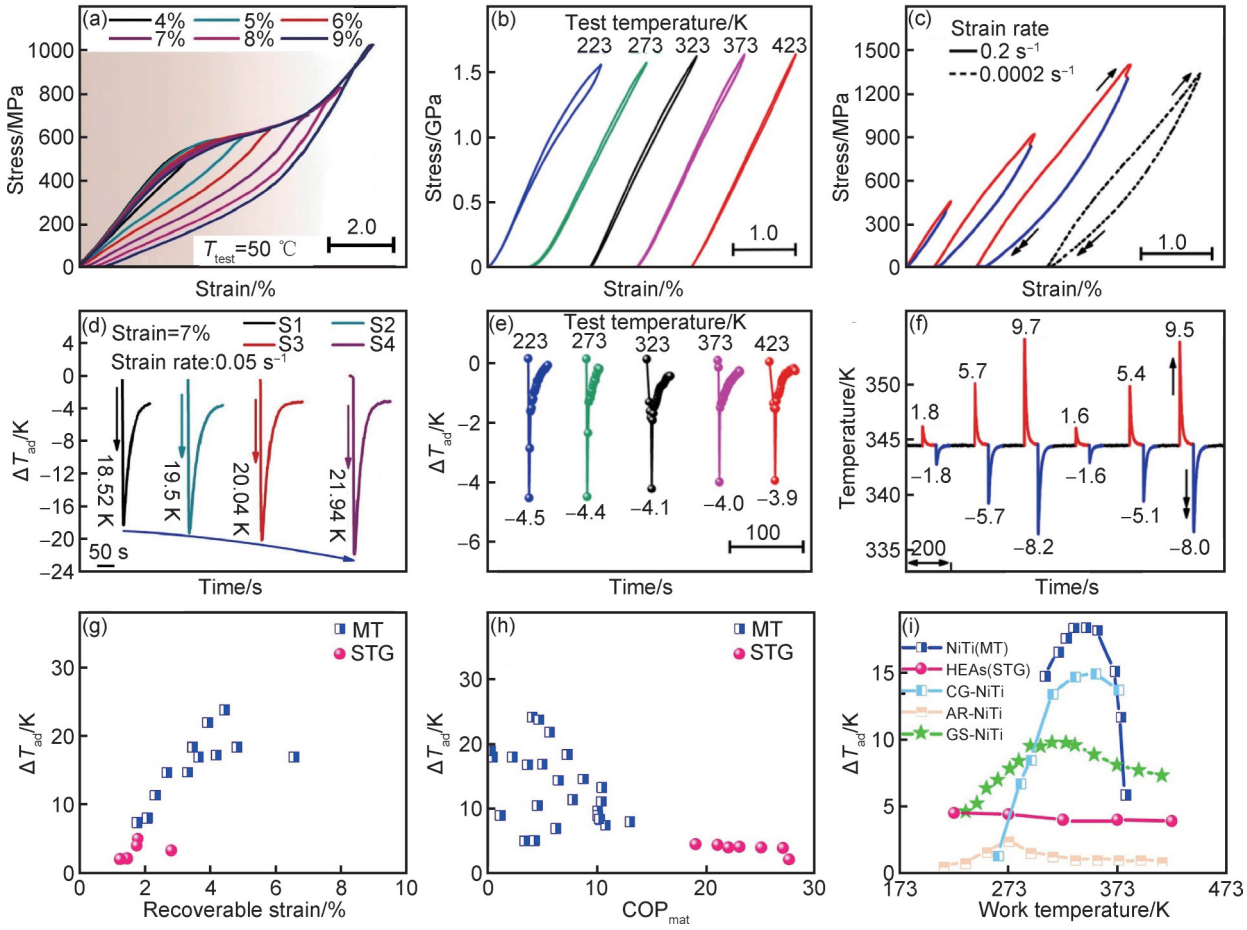


图8 马氏体相变和应变玻璃转变对应的压缩曲线和弹热性能

发生马氏体相变Ni-Ti合金(a)[115]、发生应变玻璃转变的高熵合金(b)[96]、同时发生马氏体相变和应变玻璃转变的$Ni_{55}Ti_{45}$合金(c)[55]的压缩曲线；(d)～(f)分别对应于图(a)～(c)的绝热温变[55,96,115]；(g)～(i)形状记忆合金发生马氏体相变和应变玻璃转变对应弹热性能的比较(CG：粗晶，AR：冷轧态，GS：梯度微结构)[2,96,115,133-136]

Fig.8 Compressive curves and elastocaloric properties corresponding to the martensitic transformation and strain glass transition

Compressive curves of Ni-Ti alloy undergoing martensitic transformation(a)[115], high-entropy alloys undergoing strain glass transition(b)[96], and $Ni_{55}Ti_{45}$ alloy simultaneously undergoing both martensitic transformation and strain glass transition(c)[55]; (d)-(f)the corresponding adiabatic temperature change for Fig.(a)-(c), respectively[55,96,115]; (g)-(i)comparison of elastocaloric properties corresponding to martensitic transformation and strain glass transition in shape memory alloys (CG: coarse-grained, AR: as-rolled, GS: gradient-structured)[2,96,115,133-136]

5 结束语

本文系统阐述了Ni-Ti基形状记忆合金的制备工艺、微观结构、相变行为与弹热性能之间的关联机制及最新研究进展。传统制备工艺适用于大规模生产具有良好致密度与稳定弹热性能的合金；而增材制造技术则展现出极高的设计自由度，能够实现成分与微观结构的精确调控，为开发高性能弹热制冷材料提供了新途径。通过调控晶粒形貌(如弱织构等轴晶与强织构柱状晶)、析出相(如富镍相与富钛相)以及位错、孪晶、胞状组织等亚结构，可实现对马氏体相变和应变玻璃转变的有效控制，进而提升材料的弹热制冷能力。

当前研究表明，基于马氏体相变的弹热效应虽具有较高的绝热温变，但普遍存在滞耗大、制冷效率偏低、疲劳寿命有限及工作温窗窄等问题；而基于应变

玻璃转变的体系则表现出宽工作温窗、高制冷效率与优良疲劳性能，但其绝热温变仍有待进一步提高。未来研究可从以下方面深入展开：(1)多缺陷协同调控相变路径：协调点缺陷、线缺陷与体缺陷的引入与分布，实现马氏体相变、应变玻璃转变的可控调制。(2)多尺度结构一体化设计：发展“成分-结构-性能”一体化设计策略，构建具有梯度组织、多相复合等特征的异构材料体系。(3)工艺-性能联动优化与集成：建立工艺参数-微观结构-弹热性能的定量关联与预测模型，推动制备工艺的标准化与可重复性。通过上述方向的持续探索，有望推动Ni-Ti基形状记忆合金弹热制冷技术从材料研究走向工程应用，为实现高效、环保的固态制冷提供切实可行的材料解决方案。

参考文献

[1] Leiji L, Shiyu H, Fei X, et al. Cooling innovations: elastocaloric shape memory alloys, manufacturing, simulation, and refrigerator [J]. Progress in Materials Science, 2025: 101477.1-101477.78.

[2] Qin Y X, Qin B C, Wang D Y, et al. Solid-state cooling: thermoelectrics [J]. Energy & Environmental Science, 2022, 15 (11): 4527-4541.

[3] 李冠奇，张东升，郑嘉兴，等. 激光增材制造金属功能材料及其原位同步辐射研究[J]. 中国激光，2024，51(10)：68-88.
Li G Q, Zhang D S, Zheng J X, et al. Laser additive manufacturing of metallic functional materials and *in-situ* synchrotron radiation research[J]. Chinese Journal of Lasers, 2024, 51(10): 68-88.

[4] Lu N H, Chen C H. Inhomogeneous martensitic transformation behavior and elastocaloric effect in a bicrystal Cu-Al-Mn shape memory alloy[J]. Materials Science and Engineering: A, 2021, 800: 140386.

[5] 杨院霞，千佳祥，张江，等. 硼元素对CuAlNiMn形状记忆合金微观组织与力学性能的影响[J]. 材料工程，2024，52(10)：70-79.
Yang Y X, Qian J X, Zhang J, et al. Effects of B addition on microstructure and mechanical properties of CuAlNiMn shape memory alloy[J]. Journal of Materials Engineering, 2024, 52(10): 70-79.

[6] 刘艳芬，郎子锐，李爽. Ni-Mn-Ga-Fe合金纤维的马氏体相变与超弹性[J]. 材料工程，2023，51(6)：120-130.
Liu Y F, Lang Z R, Li S. Martensitic transformation and superelasticity of Ni-Mn-Ga-Fe alloy microwires [J]. Journal of Materials Engineering, 2023, 51(6): 120-130.

[7] Yang J J, Wang H L, Li Z B, et al. Crystallography of stress-induced martensitic transformation and giant elastocaloric effect in a textured $Ni_{27}Cu_{21}Mn_{46}Sn_6$ shape memory alloy[J]. Acta Materialia, 2024, 263: 119546.

[8] Xiao F, Fukuda T, Kakeshita T, et al. Elastocaloric effect by a weak first-order transformation associated with lattice softening in an Fe-31.2Pd (at.%) alloy[J]. Acta Materialia, 2015, 87: 8-14.

[9] Xiao F, Bucsek A, Jin X J, et al. Giant elastic response and ultrastable elastocaloric effect in tweed textured Fe-Pd single crystals [J]. Acta Materialia, 2022, 223: 117486.

[10] Imran M, Zhang X X. Recent developments on the cyclic stability in elastocaloric materials [J]. Materials & Design, 2020, 195: 109030.

[11] 陈薇玫，姜浩，蒲泽，等. NiTi基形状记忆合金弹热制冷研究进展[J/OL]. 材料工程，2025：1-20. https://link.cnki.net/urlid/11.1800.TB.20250619.1542.002.
Chen W M, Jiang H, Pu Z, et al. Research progress in elastocaloric refrigeration of NiTi-based shape memory alloys [J/OL]. Journal of Materials Engineering, 2025: 1-20. https://link.cnki.net/urlid/11.1800.TB.20250619.1542.002.

[12] 吉威. NiTi形状记忆合金真空感应熔炼工艺研究[J]. 机械工程材料，1997，21(2)：50-51.
Ji W. Study of vacuum induction melting process of NiTi shape memory alloy[J]. Materials for Mechanical Engineering, 1997, 21(2): 50-51.

[13] 周剑杰，马凤仓，刘平，等. 热处理对镍钛合金表面性能的影响[J]. 有色金属材料与工程，2019，40(6)：6-13.
Zhou J J, Ma F C, Liu P, et al. Effect of heat treatment on surface properties of NiTi alloy[J]. Nonferrous Metal Materials and Engineering, 2019, 40(6): 6-13.

[14] Khaleghi F, Khalil-Allafi J, Abbasi-Chianeh V, et al. Effect of short-time annealing treatment on the superelastic behavior of cold drawn Ni-rich NiTi shape memory wires [J]. Journal of Alloys and Compounds, 2013, 554: 32-38.

[15] Weinert K, Petzoldt V. Machining of NiTi based shape memory alloys [J]. Materials Science and Engineering: A, 2004, 378(1/2): 180-184.

[16] 席瑞. 激光粉末床熔融原位制备NiTi-Nb、NiTiHf-Nb形状记忆合金及其组织性能研究[D]. 济南：山东大学，2024.

[17] Liu F, Li T T, Jia Z A, et al. Combination of stiffness, strength, and toughness in 3D printed interlocking nacre-like composites [J]. Extreme Mechanics Letters, 2020, 35: 100621.

[18] Gao S M, Feng Y C, Wang J J, et al. Molten pool characteristics of a nickel-titanium shape memory alloy for directed energy deposition[J]. Optics & Laser Technology, 2021, 142: 107215.

[19] DebRoy T, Wei H L, Zuback J S, et al. Additive manufacturing of metallic components-process, structure and properties [J]. Progress in Materials Science, 2018, 92: 112-224.

[20] Zhao C, Shi B, Chen S L, et al. Laser melting modes in metal powder bed fusion additive manufacturing [J]. Reviews of Modern Physics, 2022, 94(4): 045002.

[21] Liu J G, Wen P. Metal vaporization and its influence during laser powder bed fusion process [J]. Materials & Design, 2022, 215: 110505.

[22] Wei H L, Mukherjee T, Zhang W, et al. Mechanistic models for additive manufacturing of metallic components[J]. Progress in Materials Science, 2021, 116: 100703.

[23] Gan J, Duan L C, Li F, et al. Effect of laser energy density on the evolution of Ni_4Ti_3 precipitate and property of NiTi shape memory alloys prepared by selective laser melting [J]. Journal of Alloys and Compounds, 2021, 869: 159338.

[24] Narra S P, Rollett A D, Ngo A, et al. Process qualification of laser powder bed fusion based on processing-defect structure-fatigue

properties in Ti-6Al-4V[J].Journal of Materials Processing Technology,2023,311:117775.
[25] Zhu J N,Borisov E,Liang X H,et al.Predictive analytical modelling and experimental validation of processing maps in additive manufacturing of nitinol alloys[J].Additive Manufacturing,2021,38:101802.
[26] Xue L,Atli K C,Picak S,et al.Controlling martensitic transformation characteristics in defect-free NiTi shape memory alloys fabricated using laser powder bed fusion and a process optimization framework[J].Acta Materialia,2021,215:117017.
[27] Zhan J B,Wu J Z,Ma R J,et al.Effect of microstructure on the superelasticity of high-relative-density Ni-rich NiTi alloys fabricated by laser powder bed fusion[J].Journal of Materials Processing Technology,2023,317:117988.
[28] Wang X B,Yu J Y,Liu J W,et al.Effect of process parameters on the phase transformation behavior and tensile properties of NiTi shape memory alloys fabricated by selective laser melting[J].Additive Manufacturing,2020,36:101545.
[29] Jiang H,Wang X B,Xi R,et al.Size effect on the microstructure,phase transformation behavior,and mechanical properties of NiTi shape memory alloys fabricated by laser powder bed fusion[J].Journal of Materials Science & Technology,2023,157:200-212.
[30] 杨超,廖雨欣,卢海洲,等.NiTi形状记忆合金的功能特性及其应用发展[J].材料工程,2024,52(2):60-77.
Yang C,Liao Y X,Lu H Z,et al.Functional properties of NiTi shape memory alloys and their application development[J].Journal of Materials Engineering,2024,52(2):60-77.
[31] Gäumann M,Bezençon C,Canalis P,et al.Single-crystal laser deposition of superalloys:processing-microstructure maps[J].Acta Materialia,2001,49(6):1051-1062.
[32] Hunt J C,Kiker B F.Parental time devoted to children in two- and one-wage-earner families[J].Economics of Education Review,1984,3(1):75-83.
[33] Flood S C,Hunt J D.Columnar and equiaxed growth II.Equiaxed growth ahead of a columnar front[J].Journal of Crystal Growth,1987,82(3):552-560.
[34] Tao C C,Zhou G,Huang H J,et al.Research on energy dissipation and dynamic recrystallization microstructure evolution behavior of NiTi alloy during hot deformation[J].Materials Characterization,2024,208:113673.
[35] Sadrnezhaad S K,Mirabolghasemi S H.Optimum temperature for recovery and recrystallization of 52Ni48Ti shape memory alloy[J].Materials & Design,2007,28(6):1945-1948.
[36] Parvizi S,Hashemi S M,Asgarinia F,et al.Effective parameters on the final properties of NiTi-based alloys manufactured by powder metallurgy methods:a review[J].Progress in Materials Science,2021,117:100739.
[37] Ehsan Saghaian S,Nematollahi M,Toker G,et al.Effect of hatch spacing and laser power on microstructure,texture,and thermomechanical properties of laser powder bed fusion (L-PBF) additively manufactured NiTi[J].Optics & Laser Technology,2022,149:107680.
[38] Shao W P,He B,Qiu C Y,et al.Effect of hatch spacing and laser remelting on the formation of unique crystallographic texture of IN718 superalloy fabricated via laser powder bed fusion[J].Optics & Laser Technology,2022,156:108609.
[39] Chen J N,Liu Z Z,Liu C,et al.Effects of scanning strategy and scanning speed on microstructures and mechanical properties of NiTi alloys by laser powder bed fusion[J].Materials Science and Engineering:A,2024,914:147115.
[40] Zhu J H,Zhou H,Wang C,et al.A review of topology optimization for additive manufacturing:status and challenges[J].Chinese Journal of Aeronautics,2021,34(1):91-110.
[41] Xu Z Z,Guo Y T,Liu Y T,et al.The martensitic transformation behavior and shape memory effect of laser powder bed fusion NiTi alloys influenced by rare earth addition[J].Materials Science and Engineering:A,2022,848:143350.
[42] Wang X,Zhang L J,Ning J,et al.Hierarchical grain refinement during the laser additive manufacturing of Ti-6Al-4V alloys by the addition of micron-sized refractory particles [J].Additive Manufacturing,2021,45:102045.
[43] Lu B W,Cui X F,Ma W Y,et al.Promoting the heterogeneous nucleation and the functional properties of directed energy deposited NiTi alloy by addition of La_2O_3[J].Additive Manufacturing,2020,33:101150.
[44] Ferreri N C,Ghorbanpour S,Bhowmik S,et al.Effects of build orientation and heat treatment on the evolution of microstructure and mechanical properties of alloy Mar-M-509 fabricated via laser powder bed fusion[J].International Journal of Plasticity,2019,121:116-133.
[45] Zhang J Q,Bermingham M J,Otte J,et al.Ultrauniform,strong,and ductile 3D-printed titanium alloy through bifunctional alloy design[J].Science,2024,383(6683):639-645.
[46] Fu J,Li H,Song X,et al.Multi-scale defects in powder-based additively manufactured metals and alloys[J].Journal of Materials Science & Technology,2022,122:165-199.
[47] Shen F L,Pan L T,Li C C,et al.The microstructure and anisotropy of compressive behavior in NiTiCu alloy fabricated by laser powder bed fusion processing[J].Journal of Alloys and Compounds,2025,1032:181242.
[48] Qi X H,Liang X K,Wang J H,et al.Microstructure tailoring in laser powder bed fusion (L-PBF):strategies,challenges,and future outlooks[J].Journal of Alloys and Compounds,2024,970:172564.
[49] Fu J,Hu Z H,Song X,et al.Micro selective laser melting of NiTi shape memory alloy:defects,microstructures and thermal/mechanical properties[J].Optics & Laser Technology,2020,131:106374.
[50] Wang C,Tan X P,Du Z,et al.Additive manufacturing of NiTi shape memory alloys using pre-mixed powders[J].Journal of Materials Processing Technology,2019,271:152-161.
[51] Zhao C Y,Liang H L,Luo S C,et al.The effect of energy input on reaction,phase transition and shape memory effect of NiTi alloy by selective laser melting[J].Journal of Alloys and Compounds,2020,817:153288.
[52] Tan C L,Li S,Essa K,et al.Laser Powder Bed Fusion of Ti-rich TiNi lattice structures:process optimisation,geometrical integrity,

and phase transformations [J]. International Journal of Machine Tools and Manufacture, 2019, 141: 19-29.

[53] Gu D D, Ma C L, Dai D H, et al. Additively manufacturing-enabled hierarchical NiTi-based shape memory alloys with high strength and toughness [J]. Virtual and Physical Prototyping, 2021, 16(sup1): S19-S38.

[54] Otsuka K, Ren X. Physical metallurgy of Ti-Ni-based shape memory alloys [J]. Progress in Materials Science, 2005, 50(5): 511-678.

[55] Lv C, Wang K, Wang B, et al. Coexistence of strain glass transition and martensitic transformation in highly nickel-rich ferroelastic alloy with large elastocaloric effect [J]. Acta Materialia, 2024, 264: 119598.

[56] Hou H L, Simsek E, Ma T, et al. Fatigue-resistant high-performance elastocaloric materials made by additive manufacturing [J]. Science, 2019, 366(6469): 1116-1121.

[57] Shen F L, Pan L T, Ma T J, et al. The defects and compressive behavior of NiTi alloy fabricated by laser powder bed fusion under a wide process space [J]. Materials Today Communications, 2024, 41: 110252.

[58] Shen F L, Li H Q, Guo H, et al. Effect of energy density on the superelastic property of Ni-rich NiTi alloy fabricated by laser powder bed fusion [J]. Materials Science and Engineering: A, 2022, 854: 143874.

[59] Xu Z Z, Ji Y C, Liu C, et al. A polymer-like ultrahigh-strength metal alloy [J]. Nature, 2024, 633(8030): 575-581.

[60] Lu J Q, Zhang C, Liu Y, et al. NiTi alloys with simultaneous equiaxed-grain strength and columnar-grain ductility manipulated by direct energy deposition [J]. Journal of Alloys and Compounds, 2025, 1028: 180601.

[61] Yang C, Huang Z Y, Chen T, et al. Large recoverable strains with high recovery rates via cooperative regulation of texture and precipitation in additive manufactured NiTi alloy [J]. Scripta Materialia, 2024, 248: 116122.

[62] Bertsch K M, Meric de Bellefon G, Kuehl B, et al. Origin of dislocation structures in an additively manufactured austenitic stainless steel 316L [J]. Acta Materialia, 2020, 199: 19-33.

[63] Yang Y, Zhan J B, Sun Z Z, et al. Evolution of functional properties realized by increasing laser scanning speed for the selective laser melting fabricated NiTi alloy [J]. Journal of Alloys and Compounds, 2019, 804: 220-229.

[64] 宋长辉,付厚雄,严仲伟,等. 激光粉末床熔融成形内部质量缺陷及其调控方法[J]. 中国激光, 2022, 49(14): 1402801.
Song C H, Fu H X, Yan Z W, et al. Internal defects and control methods of laser powder bed fusion forming [J]. Chinese Journal of Lasers, 2022, 49(14): 1402801.

[65] Feng B, Wang C, Zhang Q Q, et al. Effect of laser hatch spacing on the pore defects, phase transformation and properties of selective laser melting fabricated NiTi shape memory alloys [J]. Materials Science and Engineering: A, 2022, 840: 142965.

[66] Wang C, Feng B, Chen J, et al. The effect of laser scanning strategy on NiTi shape memory alloys processed by laser powder bed fusion [J]. Materials Characterization, 2024, 215: 114185.

[67] Li B Q, Wang L, Wang B B, et al. Tuning the microstructure, martensitic transformation and superelastic properties of EBF_3-fabricated NiTi shape memory alloy using interlayer remelting [J]. Materials & Design, 2022, 220: 110886.

[68] Wang J, Pan Z X, Carpenter K, et al. Comparative study on crystallographic orientation, precipitation, phase transformation and mechanical response of Ni-rich NiTi alloy fabricated by WAAM at elevated substrate heating temperatures [J]. Materials Science and Engineering: A, 2021, 800: 140307.

[69] Ezaz T, Sehitoglu H, Maier H J. Energetics of twinning in martensitic NiTi [J]. Acta Materialia, 2011, 59(15): 5893-5904.

[70] Shamsujjoha M, Agnew S R, Fitz-Gerald J M, et al. High strength and ductility of additively manufactured 316L stainless steel explained [J]. Metallurgical and Materials Transactions A, 2018, 49(7): 3011-3027.

[71] Wang Y M, Voisin T, McKeown J T, et al. Additively manufactured hierarchical stainless steels with high strength and ductility [J]. Nature Materials, 2018, 17(1): 63-71.

[72] Ramirez D A, Murr L E, Martinez E, et al. Novel precipitate-microstructural architecture developed in the fabrication of solid copper components by additive manufacturing using electron beam melting [J]. Acta Materialia, 2011, 59(10): 4088-4099.

[73] Rukwied A, Ruff A W, Willard W A. Study of the cellular solidification structure in a continuously cast high purity copper [J]. Metallurgical Transactions, 1971, 2(8): 2105-2114.

[74] Barkia B, Aubry P, Haghi-Ashtiani P, et al. On the origin of the high tensile strength and ductility of additively manufactured 316L stainless steel: multiscale investigation [J]. Journal of Materials Science & Technology, 2020, 41: 209-218.

[75] Birnbaum A J, Steuben J C, Barrick E J, et al. Intrinsic strain aging, Σ3 boundaries, and origins of cellular substructure in additively manufactured 316L [J]. Additive Manufacturing, 2019, 29: 100784.

[76] Frenzel J, George E P, Dlouhy A, et al. Influence of Ni on martensitic phase transformations in NiTi shape memory alloys [J]. Acta Materialia, 2010, 58(9): 3444-3458.

[77] Li X Q, Chen H, Guo W M, et al. Improved superelastic stability of NiTi shape memory alloys through surface nano-crystallization followed by low temperature aging treatment [J]. Intermetallics, 2021, 131: 107114.

[78] Khoo Z, Liu Y, An J, et al. A review of selective laser melted NiTi shape memory alloy [J]. Materials, 2018, 11(4): 519.

[79] Sam J, Franco B, Ma J, et al. Tensile actuation response of additively manufactured nickel-titanium shape memory alloys [J]. Scripta Materialia, 2018, 146: 164-168.

[80] Yu Z L, Xu Z Z, Guo Y T, et al. Study on properties of SLM-NiTi shape memory alloy under the same energy density [J]. Journal of Materials Research and Technology, 2021, 13: 241-250.

[81] Wang X B, Speirs M, Kustov S, et al. Selective laser melting produced layer-structured NiTi shape memory alloys with high damping properties and Elinvar effect [J]. Scripta Materialia, 2018, 146: 246-250.

[82] Yang Y, Zhan J B, Li B, et al. Laser beam energy dependence of

martensitic transformation in SLM fabricated NiTi shape memory alloy[J].Materialia,2019,6:100305.
[83] Chen W L,Yang Q,Huang S K,et al.Laser power modulated microstructure evolution,phase transformation and mechanical properties in NiTi fabricated by laser powder bed fusion[J].Journal of Alloys and Compounds,2021,861:157959.
[84] Dadbakhsh S,Speirs M,Kruth J P,et al.Effect of SLM parameters on transformation temperatures of shape memory nickel titanium parts[J].Advanced Engineering Materials,2014,16(9):1140-1146.
[85] Ramachandran B,Tang R C,Chang P C,et al.Cu-substitution effect on thermoelectric properties of the TiNi-based shape memory alloys[J].Journal of Applied Physics,2013,113(20):203702.
[86] Trehern W,Hite N,Ortiz-Ayala R,et al.NiTiCu shape memory alloys with ultra-low phase transformation range as solid-state phase change materials[J].Acta Materialia,2023,260:119310.
[87] Li Z C,Zhong J,Zhang J L,et al.Toward additive manufactured crack-free NiTiCu shape memory alloys with low-hysteresis and tailorable phase transition behavior supported by theoretical design[J].Additive Manufacturing,2024,92:104386.
[88] Zuo X D,Zhang W,Chen Y,et al.Wire-based directed energy deposition of NiTiTa shape memory alloys:microstructure,phase transformation,electrochemistry,X-ray visibility and mechanical properties[J].Additive Manufacturing,2022,59:103115.
[89] Li Z H,Cai J X,Zhao Z H,et al.Local chemical inhomogeneity enables superior strength-ductility-superelasticity synergy in additively manufactured NiTi shape memory alloys[J].Nature Communications,2025,16:1941.
[90] Shayesteh Moghaddam N,Saedi S,Amerinatanzi A,et al.Achieving superelasticity in additively manufactured NiTi in compression without post-process heat treatment[J].Scientific Reports,2019,9:41.
[91] Cao Y X,Zhou X L,Cong D Y,et al.Large tunable elastocaloric effect in additively manufactured Ni-Ti shape memory alloys[J].Acta Materialia,2020,194:178-189.
[92] Zhu J N,Liu K,Riemslag T,et al.Achieving superelasticity in additively manufactured Ni-lean NiTi by crystallographic design[J].Materials & Design,2023,230:111949.
[93] Chen J Y,Liu B Q,Xing L L,et al.Toward tunable mechanical behavior and enhanced elastocaloric effect in NiTi alloy by gradient structure[J].Acta Materialia,2022,226:117609.
[94] Wang Y,Gao J H,Wu H J,et al.Strain glass transition in a multifunctional β-type Ti alloy[J].Scientific Reports,2014,4:3995.
[95] Ren Q S,Yuan C J,Du Z W,et al.Observation of strain-spin dual-glass state in all-d-metal Heusler alloy Ni_2MnTi[J].Acta Materialia,2025,292:121032.
[96] Zhang K C,Lv C,Li G Q,et al.Introducing strain glass transition into high-entropy TiZrHfNiCuCo alloys exhibiting elastocaloric effect and quasi-linear superelasticity[J].Acta Materialia,2025,294:121172.
[97] Wachtman J B,Tefft W E,Lam D G,et al.Exponential temperature dependence of Young's modulus for several oxides[J].Physical Review,1961,122(6):1754-1759.
[98] Sarkar S,Ren X,Otsuka K.Evidence for Strain Glass in the Ferroelastic-Martensitic System Ti_{50-x} Ni_{50+x}[J].Physical Review Letters,2005,95(20):205702.
[99] Liu C,Ji Y C,Ren X B.Strain glass and novel properties[J].Shape Memory and Superelasticity,2019,5(4):299-312.
[100] Zhang K C,Wang K,Wang B,et al.Observing strain glass transition in $Ti_{33}Nb_{15}Zr_{25}Hf_{25}O_2$ high entropy alloy with Elinvar effect[J].Journal of Materials Science & Technology,2024,168:16-23.
[101] Wang K,Lv C,Zhang K C,et al.Elastic modulus anomaly in a Fe-Mn-Cr-C cryogenic steel[J].Scripta Materialia,2022,221:114946.
[102] Wang D,Ji Y C,Ren X B,et al.Strain glass state,strain glass transition,and controlled strain release[J].Annual Review of Materials Research,2022,52:159-187.
[103] Wang Y,Ren X,Otsuka K,et al.Temperature-stress phase diagram of strain glass $Ti_{48.5}Ni_{51.5}$[J].Acta Materialia,2008,56(12):2885-2896.
[104] Guo C J,Yuan B,Du P,et al.Laser beam powder bed fusion of NiTiFe shape memory alloys by *in-situ* alloying:microstructural evolution and generation of strain glass[J].Virtual and Physical Prototyping,2025,20:e2438896.
[105] Lv C,Wang K,Cai Q Q,et al.Evidence for strain glass transition in a highly nickel-rich ferroelastic alloy[J].Materials Letters,2023,335:133793.
[106] Lai Y Z,Wang K,Lv C,et al.Strain glass transition in $Ni_{47.5+x}Ti_{50-x}Fe_{2.5}$ alloys[J].Journal of Alloys and Compounds,2022,929:167387.
[107] Wang W J,Ji Y C,Fang M X,et al.Reentrant strain glass transition in Ti-Ni-Cu shape memory alloy[J].Acta Materialia,2022,226:117618.
[108] Liao G Y,Chen B,Meng Q K,et al.Strain glass in defect-containing ferroelastic $Ti_{44}Ni_{51}Nb_5$ alloy[J].Rare Metals,2015,34(12):829-832.
[109] Lai Y Z,Wang Z L,Wang K,et al.Strain glass transition in $Ti_{48}Ni_{50}Co_2$ alloy[J].Materials Letters,2024,375:137244.
[110] Dong T J,Liang C X,Su Y T,et al.Phase field simulations for the crossover from sharp martensitic transformation into smooth strain glass transition by fine precipitates[J].Acta Materialia,2023,245:118634.
[111] Xu S,Pons J,Santamarta R,et al.Strain glass state in Ni-rich Ni-Ti-Zr shape memory alloys[J].Acta Materialia,2021,218:117232.
[112] Li L J,Yang Z S,Xu K F,et al.Strain glass state in $Ni_{50.3}Ti_{29.7}Hf_{20}$ high-temperature shape memory alloy[J].Scripta Materialia,2025,257:116449.
[113] Zhang J,Xue D Z,Cai X Y,et al.Dislocation induced strain glass in $Ti_{50}Ni_{45}Fe_5$ alloy[J].Acta Materialia,2016,120:130-137.
[114] Deng Z Z,Li Q,Onuki Y,et al.Multifunctional nanostructured NiTi alloy with Invar,Elinvar and Rinvar properties[J].Journal of Alloys and Compounds,2022,909:164682.
[115] Zhan J B,Li K,Ma R J,et al.Achieving fine tailoring of elastocaloric properties of laser powder bed-fused NiTi alloy via laser

beam manipulation[J]. International Journal of Machine Tools and Manufacture,2024,202:104210.

[116] Lin H Y,Hua P,Huang K,et al.Grain boundary and dislocation strengthening of nanocrystalline NiTi for stable elastocaloric cooling[J].Scripta Materialia,2023,226:115227.

[117] Lee H C,Shen J J,Chang Y T,et al.Evolutions of superelasticity and elastocaloric effect of $Ti_{50}Ni_{48}Fe_2$ and aged-hardened Ni-rich $Ti_{49.2}Ni_{49.3}Fe_{1.5}$ shape memory alloys under cyclic compressive deformation[J]. Journal of Alloys and Compounds, 2022, 893:162352.

[118] Hou R H,Xiao F,Zuo S G,et al.A macroscopically inhomogeneous stress-induced R-phase transformation in $Ti_{50}Ni_{48.5}Fe_{1.5}$ with enhanced elastocaloric effect[J].Acta Materialia,2024,278:120272.

[119] Ossmer H, Chluba C, Kauffmann-Weiss S, et al. TiNi-based films for elastocaloric microcooling:fatigue life and device performance[J].APL Materials,2016,4(6):064102.

[120] Chluba C,Ge W W,Lima de Miranda R,et al.Ultralow-fatigue shape memory alloy films[J].Science, 2015, 348(6238):1004-1007.

[121] Nyabadza A,Tamil K,Monu M C C,et al.Effect of geometry on the coefficient of performance of Ni-Ti elastocaloric parts manufactured via powder bed fusion[J].Journal of Materials Research and Technology,2024,30:6082-6091.

[122] Kordizadeh F,Safaei K,Mohajerani S,et al.Investigation of the elastocaloric effect in laser powder bed fusion NiTi porous structures[J].Additive Manufacturing Letters,2023,6:100131.

[123] Peng X,Yuan L H,Dai D H,et al.Novel class of additive manufactured NiTi-based hierarchically graded chiral structure with low-force compressive actuation for elastocaloric heat pumps[J]. Chinese Journal of Mechanical Engineering: Additive Manufacturing Frontiers,2023,2(2):100077.

[124] Zhan J B,Li Y,Guo Z X,et al.A 4D-printed NiTi alloy with encoded microstructures evades the cooling capacity-energy efficiency trade-off in elastocaloric refrigeration[J]. Materials Science and Engineering:R:Reports,2026,169:101191.

[125] Tan C L, Zou J, Li S, et al. Additive manufacturing of bio-inspired multi-scale hierarchically strengthened lattice structures [J]. International Journal of Machine Tools and Manufacture, 2021,167:103764.

[126] Hou H L, Cui J, Qian S X, et al. Overcoming fatigue through compression for advanced elastocaloric cooling[J]. MRS Bulletin,2018,43(4):285-290.

[127] Yu C,Kang G Z,Kan Q H,et al.Rate-dependent cyclic deformation of super-elastic NiTi shape memory alloy: thermo-mechanical coupled and physical mechanism-based constitutive model[J].International Journal of Plasticity,2015,72:60-90.

[128] Yao S J,Dang P F,Li Y M,et al.Efficient roller-driven elastocaloric refrigerator[J].Nature Communications,2024,15:7203.

[129] Wang D,Hou S,Wang Y,et al.Superelasticity of slim hysteresis over a wide temperature range by nanodomains of martensite[J]. Acta Materialia,2014,66:349-359.

[130] Ji Y C,Wang D,Wang Y,et al.Ferroic glasses[J].npj Computational Materials,2017,3:43.

[131] Zhou Y M,Xue D Z,Ding X D,et al.High temperature strain glass transition in defect doped Ti-Pd martensitic alloys[J]. Physica Status Solidi (b),2014,251(10):2027-2033.

[132] Qian Y,Wang W J,Wang Y,et al.Crossover strain glass alloy exhibiting large recoverable strain over a wide temperature range [J].Acta Materialia,2025,283:120533.

[133] Chen J Y,Wang W Q,Zhang Q,et al.Temperature dependence of elastocaloric effect in a microstructurally graded NiTi alloy[J]. Scripta Materialia,2024,245:116060.

[134] Wu Y,Ertekin E,Sehitoglu H.Elastocaloric cooling capacity of shape memory alloys-role of deformation temperatures,mechanical cycling,stress hysteresis and inhomogeneity of transformation [J].Acta Materialia,2017,135:158-176.

[135] Deng Z Z,Huang K,Yin H,et al.Temperature-dependent mechanical properties and elastocaloric effects of multiphase nanocrystalline NiTi alloys[J]. Journal of Alloys and Compounds, 2023,938:168547.

[136] 朱雪洁,钟诗江,杨晓霞,等.NiTi基形状记忆合金弹热效应及其应用研究进展[J].材料工程,2021,49(3):1-13.
Zhu X J,Zhong S J,Yang X X,et al.Research progress in elastocaloric effect and its application of NiTi-based shape memory alloys[J].Journal of Materials Engineering,2021,49(3):1-13.

基金项目:浙江省应用基础研究计划项目(2026C02A1059);国家自然科学基金面上项目(52471194);北京航空航天大学科研敢为行动计划重点项目(502GWXM2024101003);天目山实验室青年科学家项目(TK-2024-C-004);云南贵金属实验室科技计划项目(YPML-20240502098);云南省重大科技专项计划项目(202502AB080015);国家重点研发计划青年科学家项目(2022YFB3808700)

收稿日期:2026-01-22;**录用日期**:2026-05-01

通讯作者:侯慧龙(1986—),男,教授,博士,研究方向为高性能形状记忆合金制备、固态相变性能及温控技术,联系地址:浙江省杭州市余杭区瓶窑镇双红桥街166号天目山实验室(311115),E-mail:huilong_hou@buaa.edu.cn

(本文责编:齐书涵)